

Wild-Time: A Benchmark of in-the-Wild Distribution Shift over Time

Huaxiu Yao^{1*}, Caroline Choi^{1*}, Bochuan Cao², Yoonho Lee¹, Pang Wei Koh¹, Chelsea Finn¹
¹Stanford University, ²Pennsylvania State University
 wildtime@googlegroups.com

Abstract

Distribution shift occurs when the test distribution differs from the training distribution, and it can considerably degrade performance of machine learning models deployed in the real world. *Temporal shifts* – distribution shifts arising from the passage of time – often occur gradually and have the additional structure of timestamp metadata. By leveraging timestamp metadata, models can potentially learn from trends in past distribution shifts and extrapolate into the future. While recent works have studied distribution shifts, temporal shifts remain underexplored. To address this gap, we curate Wild-Time, a benchmark of 5 datasets that reflect temporal distribution shifts arising in a variety of real-world applications, including patient prognosis and news classification. On these datasets, we systematically benchmark 13 prior approaches, including methods in domain generalization, continual learning, self-supervised learning, and ensemble learning. We use two evaluation strategies: evaluation with a fixed time split (Eval-Fix) and evaluation with a data stream (Eval-Stream). Eval-Fix, our primary evaluation strategy, aims to provide a simple evaluation protocol, while Eval-Stream is more realistic for certain real-world applications. Under both evaluation strategies, we observe an average performance drop of 20% from in-distribution to out-of-distribution data. Existing methods are unable to close this gap. Code is available at <https://wild-time.github.io/>.

1 Introduction

Distribution shift occurs when the test distribution differs from the training distribution. *Temporal shifts* – distribution shifts that arise from the passage of time – are a common type of distribution shift. Due to non-stationarity, production (i.e. test) data shifts over time [39]. This degrades the performance of machine learning systems deployed in the real world. For example, Lazaridou et al. [60] found that neural language models perform worse when predicting future utterances from beyond their training period, and that their performance worsens with time. As another example, flu incidence prediction from Internet search queries performed remarkably well in 2008 [27]. However, using the same model in 2013 incorrectly predicted double the

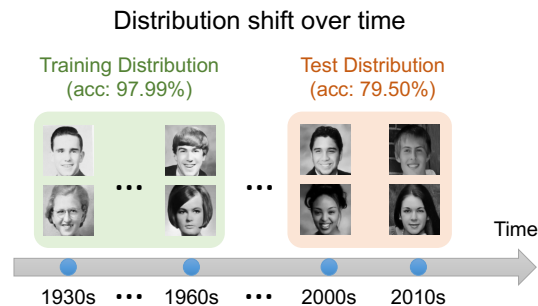


Figure 1: An illustration of temporal distribution shift on Yearbook. In Wild-Time, we split the train and test sets by timestamp and observe performance drops between train and test distributions.

*Huaxiu Yao and Caroline Choi contributed equally.



Datasets	Yearbook	FMoW-Time	MIMIC-IV		HuffPost	arXiv
			Readmission	Mortality		
Input (x)	yearbook photos	satel. image	diagnosis, treatment (ICD9)		article headline	paper title
Prediction (y)	gender	land use	readmission	mortality	news tag	primary category
Time Range	1930 - 2013	2002 - 2017	2008 - 2019		2012 - 2018	2007 - 2022
# Examples	37,189	118,886	270,617		63,907	2,057,952
Time	<div style="display: flex; justify-content: space-between;"> <div style="width: 15%;"> <p>Train Example</p>  <p>Female Residential</p> </div> <div style="width: 30%;"> <p>Diagnosis: 560, 998, 788, 278, E878, 311, V88, V10, 266, 272</p> <p>Treatment: 456, 545</p> <p>Readmission: No; Mortality: No</p> </div> <div style="width: 15%;"> <p>Killer Fail: How Romney's Broken Orca App Cost Him Thousand of Votes</p> <p>TECH</p> </div> <div style="width: 25%;"> <p>The Limitations of Deep Learning in Adversarial Settings</p> <p>cs.CR</p> </div> </div>					
	<div style="display: flex; justify-content: space-between;"> <div style="width: 15%;"> <p>Test Example</p>  <p>Female Park</p> </div> <div style="width: 30%;"> <p>Diagnosis: 155, 456, 452, 572</p> <p>Treatment: 423, 549, 990, 990</p> <p>Readmission: Yes; Mortality: Yes</p> </div> <div style="width: 15%;"> <p>Possible Autopilot Use Probed After Tesla Crashes at 60mph</p> <p>TECH</p> </div> <div style="width: 25%;"> <p>Progressive-Scale Boundary Blackbox Attack via Projective Gradient Estimation</p> <p>cs.LG</p> </div> </div>					

Figure 2: The Wild-Time benchmark includes a collection of 5 datasets with 6 tasks, from [26], [48], [76], [17]. For each task, we train models on the past and evaluate it in the future. We list the input, prediction, time range and the number of examples for each task.

incidence [8]. Finally, in Figure 1, the style of yearbook portraits of American high schoolers [26] change over the decades. As a result, models trained on earlier years and evaluated on future years suffer substantial drops in performance.

Though temporal shifts are ubiquitous in real-world scenarios, they remain understudied. Prior benchmarks for out-of-distribution robustness in the wild focus on domain shifts and subpopulation shifts [55, 72, 109, 89]. Many popular benchmarks that feature a stream of data, such as those used in continual learning [1, 13, 54, 92, 111, 14, 69, 84, 95], contain a manually delineated set of tasks and artificial sequential variations, which are not representative of natural temporal shifts. These include small-image sequences with disparate label splits (e.g., Split TinyImageNet [61], Split CIFAR [57]), different kinds of image transformations to MNIST digits (e.g., Rainbow MNIST [23]), or different visual recognition targets [64] (cf. Section 6.) Recent works have investigated natural temporal distribution shifts in different domains such as drug discovery [37], visual recognition [10], and sepsis prediction [30] and created datasets in each of these domains. However, there does not exist a systematic study of real-world temporal distribution shifts and a benchmark spanning various domains. Here, we curate a collection of these datasets and create a benchmark that allows researchers to easily evaluate their methods across multiple domains.

This paper presents **Wild-Time** (“in-the-Wild distribution shifts over Time”), a benchmark of in-the-wild gradual temporal distribution shifts together with two comprehensive evaluation protocols. In Wild-Time, we investigate real-world temporal distribution shifts across a diverse set of tasks (Figure 2), including portraits classification [26], ICU patient readmission prediction [48], ICU patient mortality prediction [48], news tag classification [76], and article category classification [17]. The distribution shifts in these applications happen naturally due to the passage of time, which the datasets reflect through changing fashion and social norms [26], atmospheric conditions [72], and current events [75, 76]. We propose two evaluation strategies for Wild-Time: evaluation with a fixed time split (Eval-Fix) and with a data stream (Eval-Stream).

On these datasets, we evaluate several representative approaches in continual learning, invariant learning, self-supervised learning, and ensemble learning. We extend invariant learning methods to the temporal distribution shift setting. While prior invariant learning approaches are trained on clearly delineated sets of distributions, we consider a stream of unsegmented observations, where domain labels are not provided. To extend domain invariant methods to the temporal distribution shift setting, we construct domains to be different windows of time. More specifically, all temporal windows of a certain window size are treated as a domain, allowing us to directly apply invariant learning approaches over the constructed domains.

The main conclusions of our benchmark analysis are that invariant learning, self-supervised learning, and continual learning approaches do not show substantial improvements compared to standard ERM training. To make the Wild-Time datasets accessible for future research, we released a Python

package that automates data loading and baseline training at <https://wild-time.github.io/>. We hope that Wild-Time will accelerate the development of temporally robust models.

2 Problem and Evaluation Settings

We define the temporal robustness setting. Following [55], we view the entire data distribution as a mixture of T timestamps $\mathcal{T} = \{1, \dots, T\}$. Each timestamp t is associated with a data distribution P_t over (x, y) , where x and y represent input features and labels, respectively, and all examples are sampled from the data distribution P_t . To formulate the temporal distribution shift setting, we define the training distribution as $P^{tr} = \sum_{t=1}^T \lambda_t^{tr} P_t$, and the test distribution as $P^{ts} = \sum_{t=1}^T \lambda_t^{ts} P_t$. Note that, here, timestamp differs from the notion of “domain” used in other works on distribution shift [24, 63, 3, 2, 55, 108]. In the temporal shift setting, we do not require distribution shift between consecutive timestamps, i.e., we can have $P_t = P_{t-1}$. Based on the problem setting, we will detail the criteria to select datasets and the evaluation strategies in Wild-Time.

2.1 Criteria for Dataset Selection

In Wild-Time, we select datasets using three criteria:

- **Naturally Occurring Temporal Shifts.** We select real-world datasets that consist of data collected over time and contain timestamp metadata. We select datasets for which it is natural to train on the past and test into the future, and we include datasets from a diverse collection of domains, including vision, healthcare, and language modeling.
- **Temporal Distribution Shifts with Performance Drops.** We require that there is substantial performance degradation between the training and test splits, i.e., we observe large drops in performance between the in-distribution and out-of-distribution times.
- **Gradual Temporal Distribution Shifts.** Sudden shifts are well-represented by existing benchmarks on domain shift and subpopulation shift. Models can more effectively extrapolate temporal correlations when the distribution shifts occur gradually over time, as opposed to sudden shifts. Thus, in this paper, we focus on gradual temporal distribution shifts, where we require gradual performance drops between consecutive periods of time.

2.2 Evaluation Strategies

Before presenting the datasets, we first discuss two evaluation strategies in Wild-Time.

Evaluation with a fixed time split (Eval-Fix). Eval-Fix evaluates models on a single, fixed train-test time split and offers a simple and quick evaluation protocol. Eval-Fix is the primary evaluation strategy in Wild-Time. Concretely, we denote the split timestamp as t_s . The train and test sets are $\mathcal{T}^{tr} = \{t \leq t_s | \forall t\}$, $\mathcal{T}^{ts} = \{t > t_s | \forall t\}$, respectively. Eval-Fix evaluates performance using two metrics, average and worst-time performance (Avg) and worst-time performance (Worst). Specifically, let R_t denote the performance at each timestamp t . We define the average performance (Avg) and worst-time performance (Worst) as

$$\text{Avg} = \frac{1}{|\mathcal{T}^{ts}|} \sum_{t \in \mathcal{T}^{ts}} R_t, \text{Worst} = \min_{t \in \mathcal{T}^{ts}} R_t. \quad (1)$$

Here, average performance measures the overall out-of-distribution performance. Worst-time performance evaluates the model’s robustness over time.

Evaluation with data stream (Eval-Stream). Eval-Stream evaluates models at each timestamp, evaluating average and worst-time performance on the next K timestamps. Eval-Stream mimics standard machine learning development pipelines, where models are updated frequently and evaluated on timestamps in the near future.

Specifically, we construct a performance matrix $\mathcal{R} \in \mathbb{R}^{T \times K}$, where each element $R_{i,j}$ is the test accuracy of the model trained on timestamp t_i and evaluated on timestamp t_j . Following [69], we define the average performance ($\text{Avg}_{\text{stream}}$) and worst-time performance ($\text{Worst}_{\text{stream}}$) as

$$\text{Avg}_{\text{stream}} = \frac{1}{|\mathcal{T}|K} \sum_{t \in \mathcal{T}} \sum_{j=t+1}^{t+K} R_{i,j}, \text{Worst}_{\text{stream}} = \frac{1}{|\mathcal{T}|} \sum_{t \in \mathcal{T}} \min_{j \in \{t+1, \dots, t+K\}} R_{i,j} \quad (2)$$

Here, K is a hyperparameter. Compared with typical continual learning metrics in Lopez-Paz and Ranzato [69], we evaluate performance on the next few timestamps, rather than just the subsequent timestamp, to assess the model’s robustness across time.

3 Datasets

In this section, we briefly discuss the datasets and tasks included in Wild-Time, which reflect natural gradual temporal distribution shifts. We provide more detailed descriptions of all datasets in Appendix A. Additionally, in Appendix F, we discuss some datasets that violate our criteria of dataset selection discussed in Section 2.1, e.g., datasets with sudden temporal distribution shifts.

Yearbook (Appendix A.1). Social norms, fashion styles, and population demographics change over time. This is captured in the Yearbook dataset, which consists of 37,921 frontal-facing American high school yearbook photos [26]. We exclude portraits from 1905 – 1929 due to the limited number of examples in these years, resulting in 33,431 examples from 1930 – 2013. Each photo is a $32 \times 32 \times 1$ grey-scale image associated with a binary label y , which represents the student’s gender. In Eval-Fix, the training set consists of data from before 1970, and the test set comprises data after 1970, which corresponds to 40 and 30 years, respectively.

FMoW-Time (Appendix A.2). Machine learning models can be used to analyze satellite imagery and aid humanitarian and policy efforts by monitoring croplands [44] and predicting crop yield [93] and poverty levels [42]. Due to human activity, satellite imagery changes over time, requiring models that are robust to temporal distribution shifts.

We study this problem on the Functional Map of the World (FMoW) dataset [16], adapted from the WILDS benchmark [55] and is named as FMoW-Time. Given a satellite image, the task is to predict the type of land usage. The FMoW-Time dataset [55] consists of 141,696 examples from 2002 – 2017. Each input x is a 224×224 RGB satellite image, and the corresponding label y is one of 62 land use categories. We use the train/val/test splits in WILDS to construct FMoW-Time dataset in Wild-Time. The train/val/test data splits from WILDS contain images from disjoint location coordinates, and all splits contain data from all 5 geographic regions. In Eval-Fix, the training set includes data from 2002 – 2015, and the test set includes data from 2016 – 2017.

MIMIC-IV (Appendix A.3). Many machine learning healthcare applications have emerged in the last decade, such as predicting disease risk [70], medication changes [105], patient subtyping [5], in-hospital mortality [30], and length of hospital stay [20]. However, changes in healthcare over time, such as the emergence of new treatments and changes in patient demographics, are an obstacle in deploying machine learning-based clinical decision support systems [30].

We study this problem on MIMIC-IV, one of the largest public healthcare datasets that comprises abundant medical records of over 40,000 patients. In MIMIC-IV, we treat each admission as one record, resulting in 216,487 healthcare records from 2008 – 2019. To protect patient privacy, the reported admission year is in a three year long date range. Hence, our timestamps are groups of three years: 2008 – 2010, 2011 – 2013, 2014 – 2016, 2017 – 2019. We consider two classification tasks:

- **MIMIC-Readmission** aims to predict the risk of being readmitted to the hospital within 15 days.
- **MIMIC-Mortality** aims to predict in-hospital mortality for each patient.

For each record, we concatenate the corresponding ICD9 codes [80] of diagnosis and treatment. A binary indicator is used to indicate the codes are come from diagnosis or treatment. We use the concatenated one as the input feature. The label is a binary value that indicates whether the patient is readmitted or passed away for MIMIC-Readmission and MIMIC-Mortality, respectively. For the Eval-Fix setting, the train set consists of patient data fom 2008 – 2013, while the test set consists of data from 2014 – 2020.

Huffpost (Appendix A.4). In many language models which deal with information correlated with time, temporal distribution shifts cause performance degradation in downstream tasks such as Twitter hashtag classification [45] or question-answering systems [66]. Performance drops across time reflect changes in the style or content of current events.

We study this temporal shift on the Huffpost dataset [76]. The task is to identify tags of news articles from their headlines. Each input feature x is a news headline, and the output y is the news category.

We only keep categories that appear in all years from 2012 – 2022, resulting 11 categories in total. We choose year 2015 as the split timestamp in Eval-Fix.

arXiv (Appendix A.5). Due to the evolution of research fields, the style of arXiv pre-prints also changes over time, reflected by the change in article categories. For example, “neural network attack” was originally a popular keyword in the security community, but gradually became more prevalent in the machine learning community. We study this temporal shift in the arXiv dataset [18], where the task is to predict the primary category of arXiv pre-prints given the paper title as input. The entire dataset includes 172 pre-print categories from 2007 – 2022.

4 Baselines for Temporal Distribution Shifts

Many algorithms have been proposed to improve a model’s robustness to distribution shifts or improve a model’s performance on a stream of data. For our evaluation, we choose several representative methods from five main categories: classical supervised learning (empirical risk minimization), continual learning, invariant learning, self-supervised learning, and ensemble learning. These methods have been successful on domain generalization and continual learning benchmarks. We extend the selected invariant learning approaches to the temporal distribution shift setting. See Appendix B for a detailed discussion of these algorithms and how we apply them to our tasks.

Classical Supervised Learning (Appendix B.1). We evaluate the performance of empirical risk minimization (ERM) on all tasks. In Eval-Fix, we directly train a machine learning model with ERM. In Eval-Stream, we apply ERM to every timestamp and report the performance.

Continual Learning (Appendix B.2). Continual learning, also known as lifelong learning or incremental learning, aims to effectively learn from non-stationary distributions via a stream of data [1, 13, 54, 92, 111, 14, 69, 84, 95]. The goal is to accumulate and reuse knowledge in future learning without forgetting information needed for previous tasks, a phenomenon known as catastrophic forgetting [54], which may enable such models to robustly extrapolate into the future in the temporal shift setting. We evaluate four representative algorithms, including fine-tuning, regularization-based (EWC, SI) and memory-based (A-GEM) methods. These methods have been successful on several continual learning benchmarks, such as permuted MNIST [28] and Split TinyImagenet [61].

Temporally Invariant Learning (Appendix B.3). Invariant learning methods learn representations or predictors that are invariant across different domains. Common approaches include aligning feature representation over different domains [24, 68, 96, 99, 104, 110, 115], learning invariant predictors via selective augmentation [108] or by strengthening the correlations between representations and labels [2, 3, 53, 58], and optimizing worst-group performance [88, 113, 114]. In Wild-Time, we select four representative invariant learning methods: CORAL [96], IRM [3], LISA [108], and GroupDRO [88]. We adapt these methods to a temporal setting and train them incrementally at each timestamp t . In the following, we discuss how we adapt these approaches to the temporal shift setting.

As mentioned in Section 2, in the temporal shift setting, the “timestamp” information is not the same as the notion of a “domain,” as the distribution shift may not occur between consecutive timestamps. The data streams in our benchmark are unsegmented and do not include domain boundaries. This setting poses new challenges to the above invariant learning approaches, which rely on domain labels.

To address this challenge, we adapt the above invariant learning approaches to the temporal distribution shift setting. We leverage timestamp metadata to create a temporal robustness set consisting of substreams of data, where each substream is treated as one domain. Specifically, as shown in Figure 3, we define a sliding window \mathcal{G} with length L . For a data stream with T timestamps, we apply the sliding window \mathcal{G} to obtain $T - L + 1$ substreams. We treat each substream as a “domain” and apply the above invariant algorithms on the robustness set. We name the adapted CORAL, GroupDRO and IRM as CORAL-T, GroupDRO-T, IRM-T, respectively. Note that we do not adapt LISA since the intra-label LISA performs well without domain information, which is also mentioned in the original paper.

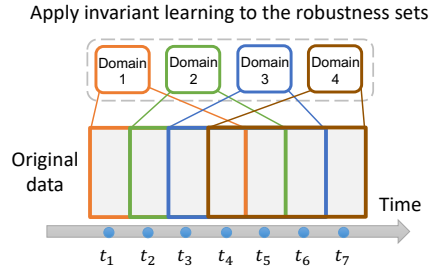


Figure 3: Construction of a temporal robustness set. Here, we have $T = 7$ and $L = 3$. By applying sliding window-based segmentation, we obtain 4 substreams of data. We apply invariant learning approaches to this robustness set.

See Appendix E.2 for details on the temporal adaptation of these invariant learning algorithms and additional ablations. In particular, we compare vanilla invariant learning algorithms with their temporally adapted versions, assess the effect of the length of the time window L , and compare performance using overlapping versus non-overlapping time windows.

Self-Supervised Learning (Appendix B.4). Self-supervised learning has been shown to improve out-of-distribution robustness [43, 94]. Here, we introduce two representative self-supervised learning methods, SimCLR [15] and SwaV [11], and evaluate their performance on the Wild-Time image classification datasets, Yearbook and FMoW-Time.

Ensemble Learning (Appendix B.5). Typically, using ensemble learning improves the performance of machine learning models. We introduce Stochastic Weighted Averaging (SWA) as the representative ensemble learning approach, which is an approximate Bayesian method which averages multiple parameter values along the trajectory of stochastic gradient descent [41].

5 Experiments

We benchmark the performance of all methods in Section 4 on each dataset in Wild-Time. Each baseline is evaluated using both the Eval-Fix and Eval-Stream settings. See Appendix D for all evaluation results and experimental details under the Eval-Stream setting.

5.1 Experimental Setup

Data Split. For both Eval-Fix and Eval-Stream, the training and test sets are subsets of the entire dataset such that the training timestamps are earlier than the test timestamps. We measure temporal out-of-distribution (OOD) robustness as performance on the test set. To compare out-of-distribution with in-distribution (ID) performance, we measure the average per-timestep performance on a held-out set of 10% training examples (20% for MIMIC-Mortality and MIMIC-Readmission) from each training ID timestamp. More details of our data split protocols are described in Appendix C.1.

Evaluation Metrics. We measure accuracy in most classification tasks, including Yearbook, FMoW-Time, MIMIC-Readmission, HuffPost, and arXiv. For the MIMIC-Mortality task, we use ROC-AUC due to label imbalance.

Hyperparameter Settings. For each dataset, we use the same backbone for all baselines. The choice of backbones are based on the original paper (e.g., DenseNet101 [36] for FMoW-Time [55], or the commonly used ones (e.g., DistilBERT [90] for arXiv and Huffpost). For each method, we tune hyperparameters using cross-validation with grid search. In Eval-Fix, we hold out 10% of the data of each training timestamp (20% for MIMIC-Readmission, and MIMIC-Mortality) to construct the validation set for hyperparameter tuning. Here, we use examples from the remaining 90% of the data to train the model and evaluate the performance on the corresponding validation set. We repeat this process three times via cross-validation with different held-out 10% of the data. After selecting all hyperparameters, we use the entire training set to train the model. See Appendix C.2 for a detailed hyperparameter search setting.

5.2 Performance Drops from Temporal Distribution Shifts

The Wild-Time datasets should exhibit observable performance drops between training and test times. In this section, we demonstrate this for every Wild-Time dataset. Table 1 shows the ID and OOD performance of ERM on each Wild-Time dataset. (See Table 20 in the Appendix for comprehensive results on all remaining baselines.)

We observe that OOD performance is substantially lower than ID performance. We conduct further experiments, in which we train ERM on both ID and OOD examples, in Appendix E.1. The substantial drop in ID versus OOD performance indicates that the performance drop is caused by distribution shift rather than the difficulty of training timestamps.

5.3 Baseline Comparison

Table 2 shows the performance of all methods on Wild-Time under the Eval-Fix setting. Due to space constraints, we report results on the Eval-Stream setting in Appendix D. We report the average

Table 1: The in-distribution versus out-of-distribution test performance evaluated on Wild-Time under the Eval-Fix setting. For each dataset, higher value means better performance.

Dataset (Metric)	In-distribution	Out-of-distribution
Yearbook (Acc)	97.99 (1.40)	79.50 (6.23)
FMoW-Time (Acc)	58.07 (0.15)	54.07 (0.25)
MIMIC-Readmission (Acc)	73.00 (2.94)	61.33 (3.45)
MIMIC-Mortality (AUC)	90.89 (0.59)	72.89 (8.96)
Huffpost (Acc)	79.40 (0.05)	70.42 (1.15)
arXiv (Acc)	53.78 (0.16)	45.94 (0.97)

Table 2: The out-of-distribution test performance of each method evaluated on Wild-Time under the Eval-Fix setting. Different groups of rows correspond to different categories of methods. Full table with standard deviation are computed over three random seeds and reported in Table 20 of Appendix. We bold the best OOD performance for each dataset.

	Yearbook (Accuracy (%) \uparrow)		FMoW-Time (Accuracy (%) \uparrow)		MIMIC-Readmission (Accuracy (%) \uparrow)	
	Avg.	Worst	Avg.	Worst	Avg.	Worst
Fine-tuning	81.98	69.62	44.25	37.14	62.19	59.57
EWC	80.07	66.61	44.02	36.42	66.40	64.69
SI	78.70	65.18	44.25	37.14	62.60	61.13
A-GEM	81.04	67.07	44.10	36.02	63.95	62.66
ERM	79.50	63.09	54.07	46.00	61.33	59.46
GroupDRO-T	77.06	60.96	43.87	36.60	56.12	53.12
mixup	76.72	58.70	53.67	44.57	58.82	57.30
LISA	83.65	68.53	52.33	43.30	56.90	54.01
CORAL-T	77.53	59.34	49.43	41.23	57.31	54.69
IRM-T	80.46	64.42	45.00	37.67	56.53	52.67
SimCLR	78.59	60.15	44.76	37.00	n/a	n/a
SwaV	78.38	60.73	44.92	37.17	n/a	n/a
SWA	84.25	67.90	54.06	46.01	59.10	56.54
	MIMIC-Mortality (AUC (%) \uparrow)		HuffPost (Accuracy (%) \uparrow)		arXiv (Accuracy (%) \uparrow)	
	Avg.	Worst	Avg.	Worst	Avg.	Worst
Fine-tuning	63.37	52.45	69.59	68.91	50.31	48.19
EWC	62.07	50.41	69.42	68.61	50.40	48.18
SI	61.76	50.19	70.46	69.05	50.21	48.07
A-GEM	61.78	50.40	70.22	69.15	50.30	48.14
ERM	72.89	65.80	70.42	68.71	45.94	44.09
GroupDRO-T	76.88	71.40	69.53	67.68	39.06	37.18
mixup	73.69	66.83	71.18	68.89	45.12	43.23
LISA	76.34	71.14	69.99	68.04	47.82	45.91
CORAL-T	77.98	64.81	70.05	68.39	42.32	40.31
IRM-T	76.16	70.64	70.21	68.71	35.75	33.91
SWA	69.53	60.83	70.98	69.52	44.36	42.54

and standard deviation of each method’s performance across three different random seeds. For each task, we visualize the OOD performance on every test timestamp in Figure 4, and show best ID performance over all approaches as an upper bound on temporally robust performance. The following high-level observations summarize our findings:

- In FMoW-Time, MIMIC-Readmission, and MIMIC-Mortality, model performance degrades with time (Figures 7h, 4c, 4d), as models exhibit higher OOD accuracy on timestamps closer to that of the training data. Such gradual temporal shifts correspond to our motivation in dataset selection, as discussed in Section 2.1. In Yearbook (Figure 7g), performance fluctuates significantly, with models achieving higher OOD accuracy at later timestamps (e.g., 1991 – 1996) compared to earlier timestamps (e.g., 1981 – 1986). In HuffPost and arXiv, models achieve the best performance on the earliest test timestamps. Nevertheless, there is a significant gap between the OOD performance

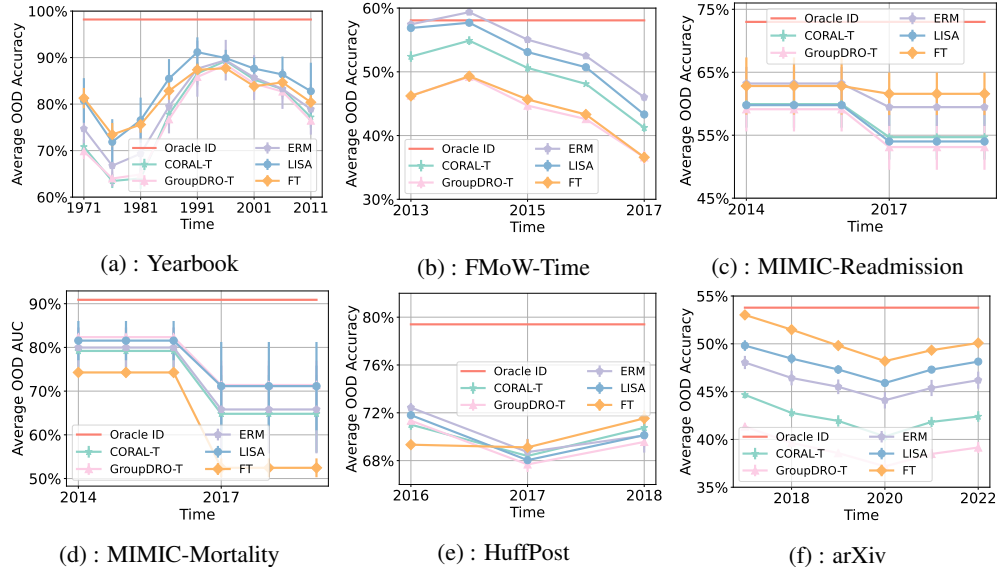


Figure 4: Out-of-distribution performance per test timestamp. We select five representative baselines – ERM, FT (Fine-tuning), CORAL-T, GroupDRO-T, LISA, and show the corresponding performance. Oracle ID represent the best ID performance over all compared baselines. Note that for MIMIC-Readmission and MIMIC-Mortality, our OOD timestamps are the three-year blocks 2014 – 2016, 2017 – 2019. Hence in Figures 4(c) and 4(d), the performance over this three-year block is the same.

and best ID performance for all datasets and methods. Furthermore, this performance gap changes in a continual manner over time, indicating that the nature of the distribution shift is correlated with the provided timestamps.

- Most invariant learning approaches (CORAL-T, GroupDRO-T, IRM-T, LISA, mixup) did not show clear improvements over ERM. In some cases, invariant learning approaches performed worse than ERM, corroborating the findings in other natural distribution shift benchmarks, such as WILDS [55].
- Incremental training approaches (Fine-tuning, EWC, SI, A-GEM) improve OOD performance on the arXiv and MIMIC-Readmission datasets, and worst OOD performance on the HuffPost dataset. This is expected, since these datasets exhibit more gradual temporal shifts, and incremental training tends to bias the trained model towards the last few timestamps. In all tasks other than Yearbook, incremental training methods perform worse than invariant learning approaches, indicating the power of invariance in learning temporally robust models.
- Neither self-supervised learning nor ensemble learning approaches show consistent benefits over ERM. In summary, ERM has been shown to be a strong baseline in Wild-Time, even when we reduce the number of training examples, as discussed in Appendix E.4.
- Most results from the Eval-Stream setting (Appendix D) concur with the above findings from the Eval-Fix setting. In particular, invariant learning approaches outperform continual learning approaches in more scenarios except FMoW-Time, Huffpost and arXiv, though we do not restrict the buffer size for invariant learning approaches. We hope that Wild-Time will be used to investigate more memory-efficient invariant learning approaches.

6 Comparison with Existing Benchmarks

Wild-Time offers a unified framework to facilitate the development of models robust to in-the-wild temporal distribution shifts. We discuss how Wild-Time is related to existing distribution shift and continual learning benchmarks.

Relation to Distribution Shift Benchmarks. Distribution shift has been widely studied in the machine learning community. Early works presented small-scale benchmarks to study distribution shifts in sentiment analysis [22] and object detection [87]. Subsequent distribution shift benchmarks focused on larger-scale, real-world data. The first line of such benchmarks induce distribution shifts

by applying different transformations to object recognition datasets. These benchmarks include: (1) ImageNet-A [35], ImageNet-C [33], and CIFAR-10.1 [85], which add noise or adversarial examples to the original Imagenet [86] and CIFAR [57] datasets, respectively; (2) Colored MNIST [3], which changes the color of digits from the original MNIST. More recent works created domain generalization benchmarks by collecting sets of images with different styles or backgrounds, such as PACS [62], DomainNet [82], VLCS [21], OfficeHome [102], ImageNet-R [34], BREEDS [91], Waterbirds [88], NICO [32], and MetaShift [65]. While these datasets are useful testbeds for verifying the efficacy of new algorithms, they do not reflect natural distribution shifts that arise in real-world applications.

Recently, a few works have constructed datasets and benchmarks for real-world distribution shifts. WILDS benchmark consists of ten datasets spanning a wide range of real-world applications, such as medical image recognition, sentiment classification, land-use classification with satellite image, and code autocompletion, with a focus on domain shifts and subpopulation shifts [55]. WILDS 2.0 extends WILDS and introduces unlabeled data to help boost model robustness to distribution shifts [89]. SHIFTS [72] is composed of three datasets, concerning weather prediction, machine translation, and self-driving vehicle motion prediction. Unlike these works that focus on general distribution shifts, we target temporal distribution shifts arising in real-world applications. A few recent works have started investigating model robustness over time, in real-world applications such as healthcare-related prediction [30], drug discovery [37], image-based geo-localization [10], machine reading comprehension [66], and tweet hashtag prediction [45]. Unlike prior datasets that target specific applications, Wild-Time presents a comprehensive benchmark comprised of 7 datasets from diverse domains and offers systematic evaluation protocols.

Relation to Continual Learning Benchmarks. Continual learning methods are often benchmarked on image classification datasets. Some popular benchmarks such as RainbowMNIST [23] and permuted MNIST [50] apply various image transformations to a small-scale image dataset to obtain a sequence of tasks. Others such as Split CIFAR100 [57], Split TinyImagenet [61], F-CelebA [51], and Stanford Cars [56] split a large image dataset into multiple non-overlapping class sets, where each is regarded as one task. A third collection of related benchmarks treats each object recognition dataset as a different task. For example, Visual Domain Decathlon [64] consists of 10 datasets from various domains, such as Aircraft [71], SVHN [77], Omniglot [59], VGG-Flowers [78], CLEAR [67]. In the natural language processing (NLP) domain, continual learning benchmarks such as ASC [52] and DSC [51] have been used to evaluate the performance of large-scale pretrained models over time. Unlike these prior benchmarks, Wild-Time presents a collection of datasets that reflect natural temporal distribution shifts arising in real-world applications as well as an evaluation strategy (Eval-Stream) to assess incremental learning approaches.

7 Conclusion and Discussion

In this paper, we present the Wild-Time benchmark, and examine in-the-wild distribution shifts over time. We leverage timestamp metadata, which is largely ignored by existing robustness techniques and benchmarks. Wild-Time includes 6 tasks from 5 datasets, which span a range of applications (facial recognition, news, healthcare) and tasks (classification, regression). On each of these datasets, we systematically benchmark 13 approaches, including continual learning, invariant learning, self-supervised learning, and ensemble learning approaches. Our experiments show a large gap between ID and OOD performance on all tasks due to temporal distribution shift. We conclude that no existing invariant learning, continual learning, self-supervised, or ensemble learning approach is consistently more robust to temporal distribution shifts than ERM. We hope that Wild-Time facilitates further research in developing temporally robust methods that can be safely deployed in the wild.

Acknowledgement

We thank Zhenbang Wu, Shiori Sagawa, Kexin Huang, Ananya Kumar, Scott Lanyon Fleming, and members of the IRIS lab for the many insightful discussions and helpful feedback. This research was funded in part by Apple, Intel, Juniper Networks, and JPMorgan Chase & Co. Any views or opinions expressed herein are solely those of the authors listed, and may differ from the views and opinions expressed by JPMorgan Chase & Co. or its affiliates. This material is not a product of the Research Department of J.P. Morgan Securities LLC. This material should not be construed as an individual recommendation for any particular client and is not intended as a recommendation of particular securities, financial instruments or strategies for a particular client. This material does not constitute a solicitation or offer in any jurisdiction. CF is a CIFAR fellow.

References

- [1] Tameem Adel, Han Zhao, and Richard E Turner. Continual learning with adaptive weights (claw). *arXiv preprint arXiv:1911.09514*, 2019.
- [2] Kartik Ahuja, Ethan Caballero, Dinghuai Zhang, Yoshua Bengio, Ioannis Mitliagkas, and Irina Rish. Invariance principle meets information bottleneck for out-of-distribution generalization. 2021.
- [3] Martin Arjovsky, Léon Bottou, Ishaan Gulrajani, and David Lopez-Paz. Invariant risk minimization. *arXiv preprint arXiv:1907.02893*, 2019.
- [4] Ben Athiwaratkun, Marc Finzi, Pavel Izmailov, and Andrew Gordon Wilson. There are many consistent explanations of unlabeled data: Why you should average. *arXiv preprint arXiv:1806.05594*, 2018.
- [5] Inci M Baytas, Cao Xiao, Xi Zhang, Fei Wang, Anil K Jain, and Jiayu Zhou. Patient subtyping via time-aware lstm networks. In *Proceedings of the 23rd ACM SIGKDD international conference on knowledge discovery and data mining*, pages 65–74, 2017.
- [6] Gabrielle Berman, Sara de la Rosa, Tanya Accone, et al. Ethical considerations when using geospatial technologies for evidence generation. 2018.
- [7] Matteo Boschini, Lorenzo Bonicelli, Pietro Buzzega, Angelo Porrello, and Simone Calderara. Class-incremental continual learning into the extended der-verse. *arXiv preprint arXiv:2201.00766*, 2022.
- [8] Declan Butler. When google got flu wrong: Us outbreak foxes a leading web-based method for tracking seasonal flu. *Nature*, 494(7436):155–157, 2013.
- [9] Pietro Buzzega, Matteo Boschini, Angelo Porrello, Davide Abati, and Simone Calderara. Dark experience for general continual learning: a strong, simple baseline. In H. Larochelle, M. Ranzato, R. Hadsell, M. F. Balcan, and H. Lin, editors, *Advances in Neural Information Processing Systems*, volume 33, pages 15920–15930. Curran Associates, Inc., 2020.
- [10] Zhipeng Cai, Ozan Sener, and Vladlen Koltun. Online continual learning with natural distribution shifts: An empirical study with visual data. In *Proceedings of the IEEE/CVF International Conference on Computer Vision*, pages 8281–8290, 2021.
- [11] Mathilde Caron, Ishan Misra, Julien Mairal, Priya Goyal, Piotr Bojanowski, and Armand Joulin. Unsupervised learning of visual features by contrasting cluster assignments. *Advances in Neural Information Processing Systems*, 33:9912–9924, 2020.
- [12] Kristy A Carpenter, David S Cohen, Juliet T Jarrell, and Xudong Huang. Deep learning and virtual drug screening. *Future medicinal chemistry*, 10(21):2557–2567, 2018.
- [13] Arslan Chaudhry, Puneet K Dokania, Thalaiyasingam Ajanthan, and Philip HS Torr. Riemannian walk for incremental learning: Understanding forgetting and intransigence. In *Proceedings of the European Conference on Computer Vision (ECCV)*, pages 532–547, 2018.
- [14] Arslan Chaudhry, Marc’Aurelio Ranzato, Marcus Rohrbach, and Mohamed Elhoseiny. Efficient lifelong learning with a-GEM. In *International Conference on Learning Representations*, 2019. URL https://openreview.net/forum?id=Hkf2_sC5FX.
- [15] Ting Chen, Simon Kornblith, Mohammad Norouzi, and Geoffrey Hinton. A simple framework for contrastive learning of visual representations. In *International conference on machine learning*, pages 1597–1607. PMLR, 2020.
- [16] Gordon Christie, Neil Fendley, James Wilson, and Ryan Mukherjee. Functional map of the world. In *Proceedings of the IEEE Conference on Computer Vision and Pattern Recognition*, 2018.
- [17] Colin B. Clement, Matthew Bierbaum, Kevin P. O’Keeffe, and Alexander A. Alemi. On the use of arxiv as a dataset, 2019.

- [18] Colin B Clement, Matthew Bierbaum, Kevin P O’Keeffe, and Alexander A Alemi. On the use of arxiv as a dataset. *arXiv preprint arXiv:1905.00075*, 2019.
- [19] Drew DeSilver. The polarization in today’s congress has roots that go back decades. 2022.
- [20] Roelof GA Ettema, Linda M Peelen, Marieke J Schuurmans, Arno P Nierich, Cor J Kalkman, and Karel GM Moons. Prediction models for prolonged intensive care unit stay after cardiac surgery: systematic review and validation study. *Circulation*, 122(7):682–689, 2010.
- [21] Chen Fang, Ye Xu, and Daniel N Rockmore. Unbiased metric learning: On the utilization of multiple datasets and web images for softening bias. In *Proceedings of the IEEE International Conference on Computer Vision*, pages 1657–1664, 2013.
- [22] Fang Fang, Kaushik Dutta, and Anindya Datta. Domain adaptation for sentiment classification in light of multiple sources. *INFORMS Journal on Computing*, 26(3):586–598, 2014.
- [23] Chelsea Finn, Aravind Rajeswaran, Sham Kakade, and Sergey Levine. Online meta-learning. In *International Conference on Machine Learning*, pages 1920–1930, 2019.
- [24] Yaroslav Ganin, Evgeniya Ustinova, Hana Ajakan, Pascal Germain, Hugo Larochelle, François Laviolette, Mario Marchand, and Victor Lempitsky. Domain-adversarial training of neural networks. *The journal of machine learning research*, 17(1):2096–2030, 2016.
- [25] Sara Gerke, Timo Minssen, and Glenn Cohen. Ethical and legal challenges of artificial intelligence-driven healthcare. In *Artificial intelligence in healthcare*, pages 295–336. Elsevier, 2020.
- [26] Shiry Ginosar, Kate Rakelly, Sarah Sachs, Brian Yin, and Alexei A Efros. A century of portraits: A visual historical record of american high school yearbooks. In *Proceedings of the IEEE International Conference on Computer Vision Workshops*, pages 1–7, 2015.
- [27] Jeremy Ginsberg, Matthew H Mohebbi, Rajan S Patel, Lynnette Brammer, Mark S Smolinski, and Larry Brilliant. Detecting influenza epidemics using search engine query data. *Nature*, 457(7232):1012–1014, 2009.
- [28] Ian J Goodfellow, Mehdi Mirza, Da Xiao, Aaron Courville, and Yoshua Bengio. An empirical investigation of catastrophic forgetting in gradient-based neural networks. *arXiv preprint arXiv:1312.6211*, 2013.
- [29] Ishaan Gulrajani and David Lopez-Paz. In search of lost domain generalization. *arXiv preprint arXiv:2007.01434*, 2020.
- [30] Lin Lawrence Guo, Stephen R Pfohl, Jason Fries, Alistair EW Johnson, Jose Posada, Catherine Aftandilian, Nigam Shah, and Lillian Sung. Evaluation of domain generalization and adaptation on improving model robustness to temporal dataset shift in clinical medicine. *Scientific reports*, 12(1):1–10, 2022.
- [31] Matthew C Hansen, Peter V Potapov, Rebecca Moore, Matt Hancher, Svetlana A Turubanova, Alexandra Tyukavina, David Thau, Stephen V Stehman, Scott J Goetz, Thomas R Loveland, et al. High-resolution global maps of 21st-century forest cover change. *science*, 342(6160): 850–853, 2013.
- [32] Yue He, Zheyang Shen, and Peng Cui. Towards non-iid image classification: A dataset and baselines. *Pattern Recognition*, 110:107383, 2021.
- [33] Dan Hendrycks and Thomas Dietterich. Benchmarking neural network robustness to common corruptions and perturbations. *arXiv preprint arXiv:1903.12261*, 2019.
- [34] Dan Hendrycks, Steven Basart, Norman Mu, Saurav Kadavath, Frank Wang, Evan Dorundo, Rahul Desai, Tyler Zhu, Samyak Parajuli, Mike Guo, et al. The many faces of robustness: A critical analysis of out-of-distribution generalization. In *Proceedings of the IEEE/CVF International Conference on Computer Vision*, pages 8340–8349, 2021.

- [35] Dan Hendrycks, Kevin Zhao, Steven Basart, Jacob Steinhardt, and Dawn Song. Natural adversarial examples. In *Proceedings of the IEEE/CVF Conference on Computer Vision and Pattern Recognition*, pages 15262–15271, 2021.
- [36] Gao Huang, Zhuang Liu, Laurens Van Der Maaten, and Kilian Q Weinberger. Densely connected convolutional networks. In *Proceedings of the IEEE conference on computer vision and pattern recognition*, pages 4700–4708, 2017.
- [37] Kexin Huang, Tianfan Fu, Wenhao Gao, Yue Zhao, Yusuf Roohani, Jure Leskovec, Connor W Coley, Cao Xiao, Jimeng Sun, and Marinka Zitnik. Therapeutics data commons: Machine learning datasets and tasks for drug discovery and development. *arXiv preprint arXiv:2102.09548*, 2021.
- [38] James P Hughes, Stephen Rees, S Barrett Kalindjian, and Karen L Philpott. Principles of early drug discovery. *British journal of pharmacology*, 162(6):1239–1249, 2011.
- [39] Chip Huyen. *Designing Machine Learning Systems*. " O'Reilly Media, Inc.", 2022.
- [40] Philipp Wirth Jeremy Prescott Malte Ebner et al. Igor Susmelj, Matthias Heller. Lightly. *GitHub*. Note: <https://github.com/lightly-ai/lightly>, 2020.
- [41] Pavel Izmailov, Dmitrii Podoprikin, Timur Garipov, Dmitry Vetrov, and Andrew Gordon Wilson. Averaging weights leads to wider optima and better generalization. *arXiv preprint arXiv:1803.05407*, 2018.
- [42] Neal Jean, Marshall Burke, Michael Xie, W Matthew Davis, David B Lobell, and Stefano Ermon. Combining satellite imagery and machine learning to predict poverty. *Science*, 353(6301):790–794, 2016.
- [43] Wenlong Ji, Zhun Deng, Ryumei Nakada, James Zou, and Linjun Zhang. The power of contrast for feature learning: A theoretical analysis. *arXiv preprint arXiv:2110.02473*, 2021.
- [44] Xiaowei Jia, Mengdie Wang, Ankush Khandelwal, Anuj Karpatne, and Vipin Kumar. Recurrent generative networks for multi-resolution satellite data: An application in cropland monitoring. In *IJCAI*, 2019.
- [45] Xisen Jin, Dejiao Zhang, Henghui Zhu, Wei Xiao, Shang-Wen Li, Xiaokai Wei, Andrew Arnold, and Xiang Ren. Lifelong pretraining: Continually adapting language models to emerging corpora. *arXiv preprint arXiv:2110.08534*, 2021.
- [46] Anna Jobin, Marcello Ienca, and Effy Vayena. The global landscape of ai ethics guidelines. *Nature Machine Intelligence*, 1(9):389–399, 2019.
- [47] Alistair Johnson, Lucas Bulgarelli, Tom Pollard, Steven Horng, Leo Anthony Celi, and Roger Mark. Mimic-iv. *version 0.4*). *PhysioNet*. <https://doi.org/10.13026/a3wn-hq05>, 2020.
- [48] Alistair Johnson, Lucas Bulgarelli, Tom Pollard, Steven Horng, Leo Anthony Celi, and Roger Mark. Mimic-iv, 2021. URL <https://physionet.org/content/mimiciv/1.0/>.
- [49] Manu Joseph. Pytorch tabular: A framework for deep learning with tabular data, 2021.
- [50] Prakhar Kaushik, Alex Gain, Adam Kortylewski, and Alan Yuille. Understanding catastrophic forgetting and remembering in continual learning with optimal relevance mapping. *arXiv preprint arXiv:2102.11343*, 2021.
- [51] Zixuan Ke, Bing Liu, Hao Wang, and Lei Shu. Continual learning with knowledge transfer for sentiment classification. In *Joint European Conference on Machine Learning and Knowledge Discovery in Databases*, pages 683–698. Springer, 2020.
- [52] Zixuan Ke, Hu Xu, and Bing Liu. Adapting bert for continual learning of a sequence of aspect sentiment classification tasks. *arXiv preprint arXiv:2112.03271*, 2021.
- [53] Kia Khezeli, Arno Blaas, Frank Soboczenski, Nicholas Chia, and John Kalantari. On invariance penalties for risk minimization. *arXiv preprint arXiv:2106.09777*, 2021.

- [54] James Kirkpatrick, Razvan Pascanu, Neil Rabinowitz, Joel Veness, Guillaume Desjardins, Andrei A Rusu, Kieran Milan, John Quan, Tiago Ramalho, Agnieszka Grabska-Barwinska, et al. Overcoming catastrophic forgetting in neural networks. *Proceedings of the national academy of sciences*, 114(13):3521–3526, 2017.
- [55] Pang Wei Koh, Shiori Sagawa, Sang Michael Xie, Marvin Zhang, Akshay Balsubramani, Weihua Hu, Michihiro Yasunaga, Richard Lanus Phillips, Irena Gao, Tony Lee, et al. Wilds: A benchmark of in-the-wild distribution shifts. In *International Conference on Machine Learning*, pages 5637–5664. PMLR, 2021.
- [56] Jonathan Krause, Michael Stark, Jia Deng, and Li Fei-Fei. 3d object representations for fine-grained categorization. In *4th International IEEE Workshop on 3D Representation and Recognition (3dRR-13)*, Sydney, Australia, 2013.
- [57] Alex Krizhevsky, Geoffrey Hinton, et al. Learning multiple layers of features from tiny images. 2009.
- [58] David Krueger, Ethan Caballero, Joern-Henrik Jacobsen, Amy Zhang, Jonathan Binas, Dinghuai Zhang, Remi Le Priol, and Aaron Courville. Out-of-distribution generalization via risk extrapolation (rex). In *International Conference on Machine Learning*, pages 5815–5826. PMLR, 2021.
- [59] Brenden M Lake, Ruslan Salakhutdinov, and Joshua B Tenenbaum. Human-level concept learning through probabilistic program induction. *Science*, 350(6266):1332–1338, 2015.
- [60] Angeliki Lazaridou, Adhi Kuncoro, Elena Gribovskaya, Devang Agrawal, Adam Liska, Tayfun Terzi, Mai Gimenez, Cyprien de Masson d’Autume, Tomas Kocisky, Sebastian Ruder, et al. Mind the gap: Assessing temporal generalization in neural language models. *Advances in Neural Information Processing Systems*, 34:29348–29363, 2021.
- [61] Ya Le and Xuan Yang. Tiny imagenet visual recognition challenge. *CS 231N*, 7(7):3, 2015.
- [62] Da Li, Yongxin Yang, Yi-Zhe Song, and Timothy M Hospedales. Deeper, broader and artier domain generalization. In *Proceedings of the IEEE international conference on computer vision*, pages 5542–5550, 2017.
- [63] Haoliang Li, Sinno Jialin Pan, Shiqi Wang, and Alex C Kot. Domain generalization with adversarial feature learning. In *Proceedings of the IEEE Conference on Computer Vision and Pattern Recognition*, pages 5400–5409, 2018.
- [64] Xilai Li, Yingbo Zhou, Tianfu Wu, Richard Socher, and Caiming Xiong. Learn to grow: A continual structure learning framework for overcoming catastrophic forgetting. *arXiv preprint arXiv:1904.00310*, 2019.
- [65] Weixin Liang and James Zou. Metashift: A dataset of datasets for evaluating contextual distribution shifts and training conflicts. *arXiv preprint arXiv:2202.06523*, 2022.
- [66] Bill Yuchen Lin, Sida Wang, Xi Victoria Lin, Robin Jia, Lin Xiao, Xiang Ren, and Wentaoh Yih. On continual model refinement in out-of-distribution data streams. *arXiv preprint arXiv:2205.02014*, 2022.
- [67] Zhiqiu Lin, Jia Shi, Deepak Pathak, and Deva Ramanan. The clear benchmark: Continual learning on real-world imagery. In *Thirty-fifth Conference on Neural Information Processing Systems Datasets and Benchmarks Track*, 2021.
- [68] Mingsheng Long, Yue Cao, Jianmin Wang, and Michael Jordan. Learning transferable features with deep adaptation networks. In *International conference on machine learning*, pages 97–105. PMLR, 2015.
- [69] David Lopez-Paz and Marc’Aurelio Ranzato. Gradient episodic memory for continual learning. In *Advances in Neural Information Processing Systems*, pages 6467–6476, 2017.

- [70] Fenglong Ma, Radha Chitta, Jing Zhou, Quanzeng You, Tong Sun, and Jing Gao. Dipole: Diagnosis prediction in healthcare via attention-based bidirectional recurrent neural networks. In *Proceedings of the 23rd ACM SIGKDD international conference on knowledge discovery and data mining*, pages 1903–1911, 2017.
- [71] S. Maji, J. Kannala, E. Rahtu, M. Blaschko, and A. Vedaldi. Fine-grained visual classification of aircraft. Technical report, 2013.
- [72] Andrey Malinin, Neil Band, German Chesnokov, Yarin Gal, Mark JF Gales, Alexey Noskov, Andrey Ploskonosov, Liudmila Prokhorenkova, Ivan Provilkov, Vatsal Raina, et al. Shifts: A dataset of real distributional shift across multiple large-scale tasks. *arXiv preprint arXiv:2107.07455*, 2021.
- [73] Eric J Martin, Valery R Polyakov, Xiang-Wei Zhu, Li Tian, Prasenjit Mukherjee, and Xin Liu. All-assay-max2 pqsar: activity predictions as accurate as four-concentration ic50s for 8558 novartis assays. *Journal of chemical information and modeling*, 59(10):4450–4459, 2019.
- [74] Ninareh Mehrabi, Fred Morstatter, Nripsuta Saxena, Kristina Lerman, and Aram Galstyan. A survey on bias and fairness in machine learning. *ACM Computing Surveys (CSUR)*, 54(6):1–35, 2021.
- [75] Rishabh Misra. News category dataset, 06 2018.
- [76] Rishabh Misra and Jigyasa Grover. *Sculpting Data for ML: The first act of Machine Learning*. 01 2021. ISBN 978-0-578-83125-1.
- [77] Yuval Netzer, Tao Wang, Adam Coates, Alessandro Bissacco, Bo Wu, and Andrew Y Ng. Reading digits in natural images with unsupervised feature learning. 2011.
- [78] Maria-Elena Nilsback and Andrew Zisserman. Automated flower classification over a large number of classes. In *2008 Sixth Indian Conference on Computer Vision, Graphics & Image Processing*, pages 722–729. IEEE, 2008.
- [79] Peter A Noseworthy, Zachi I Attia, LaPrincess C Brewer, Sharonne N Hayes, Xiaoxi Yao, Suraj Kapa, Paul A Friedman, and Francisco Lopez-Jimenez. Assessing and mitigating bias in medical artificial intelligence: the effects of race and ethnicity on a deep learning model for ecg analysis. *Circulation: Arrhythmia and Electrophysiology*, 13(3):e007988, 2020.
- [80] World Health Organization. *International Statistical Classification of Diseases and Related Health Problems: Alphabetical index*, volume 3. World Health Organization, 2004.
- [81] Hakime Öztürk, Arzucan Özgür, and Elif Ozkirimli. Deepdta: deep drug–target binding affinity prediction. *Bioinformatics*, 34(17):i821–i829, 2018.
- [82] Xingchao Peng, Qinxun Bai, Xide Xia, Zijun Huang, Kate Saenko, and Bo Wang. Moment matching for multi-source domain adaptation. In *Proceedings of the IEEE/CVF international conference on computer vision*, pages 1406–1415, 2019.
- [83] R Powers and D Beede. Fostering innovation, creating jobs, driving better decisions: The value of government data. *Office of the Chief Economist, Economics and Statistics Administration, US Department of Commerce*, 2014.
- [84] Sylvestre-Alvise Rebuffi, Alexander Kolesnikov, Georg Sperl, and Christoph H Lampert. icarl: Incremental classifier and representation learning. In *Proceedings of the IEEE conference on Computer Vision and Pattern Recognition*, pages 2001–2010, 2017.
- [85] Benjamin Recht, Rebecca Roelofs, Ludwig Schmidt, and Vaishaal Shankar. Do cifar-10 classifiers generalize to cifar-10? *arXiv preprint arXiv:1806.00451*, 2018.
- [86] Olga Russakovsky, Jia Deng, Hao Su, Jonathan Krause, Sanjeev Satheesh, Sean Ma, Zhiheng Huang, Andrej Karpathy, Aditya Khosla, Michael Bernstein, et al. Imagenet large scale visual recognition challenge. *International journal of computer vision*, 115(3):211–252, 2015.
- [87] Kate Saenko, Brian Kulis, Mario Fritz, and Trevor Darrell. Adapting visual category models to new domains. In *European conference on computer vision*, pages 213–226. Springer, 2010.

- [88] Shiori Sagawa, Pang Wei Koh, Tatsunori B Hashimoto, and Percy Liang. Distributionally robust neural networks for group shifts: On the importance of regularization for worst-case generalization. In *ICLR*, 2020.
- [89] Shiori Sagawa, Pang Wei Koh, Tony Lee, Irena Gao, Sang Michael Xie, Kendrick Shen, Ananya Kumar, Weihua Hu, Michihiro Yasunaga, Henrik Marklund, Sara Beery, Etienne David, Ian Stavness, Wei Guo, Jure Leskovec, Kate Saenko, Tatsunori Hashimoto, Sergey Levine, Chelsea Finn, and Percy Liang. Extending the wilds benchmark for unsupervised adaptation. In *International Conference on Learning Representations (ICLR)*, 2022.
- [90] Victor Sanh, Lysandre Debut, Julien Chaumond, and Thomas Wolf. Distilbert, a distilled version of bert: smaller, faster, cheaper and lighter. *arXiv preprint arXiv:1910.01108*, 2019.
- [91] Shibani Santurkar, Dimitris Tsipras, and Aleksander Madry. Breeds: Benchmarks for subpopulation shift. *arXiv preprint arXiv:2008.04859*, 2020.
- [92] Jonathan Schwarz, Wojciech Czarnecki, Jelena Luketina, Agnieszka Grabska-Barwinska, Yee Whye Teh, Razvan Pascanu, and Raia Hadsell. Progress & compress: A scalable framework for continual learning. In *International Conference on Machine Learning*, pages 4528–4537, 2018.
- [93] Alireza Sharifi. Yield prediction with machine learning algorithms and satellite images. *Journal of the Science of Food and Agriculture*, 101(3):891–896, 2021.
- [94] Kendrick Shen, Robbie M Jones, Ananya Kumar, Sang Michael Xie, Jeff Z HaoChen, Tengyu Ma, and Percy Liang. Connect, not collapse: Explaining contrastive learning for unsupervised domain adaptation. In *International Conference on Machine Learning*, pages 19847–19878. PMLR, 2022.
- [95] Hanul Shin, Jung Kwon Lee, Jaehong Kim, and Jiwon Kim. Continual learning with deep generative replay. In *Advances in Neural Information Processing Systems*, pages 2990–2999, 2017.
- [96] Baochen Sun and Kate Saenko. Deep coral: Correlation alignment for deep domain adaptation. In *European conference on computer vision*, pages 443–450. Springer, 2016.
- [97] Vladimir Svetnik, Andy Liaw, Christopher Tong, J Christopher Culberson, Robert P Sheridan, and Bradley P Feuston. Random forest: a classification and regression tool for compound classification and qsar modeling. *Journal of chemical information and computer sciences*, 43(6):1947–1958, 2003.
- [98] Tobias G. Tiecke, Xianming Liu, Amy Zhang, Andreas Gros, Nan Li, Gregory Yetman, Talip Kilic, Siobhan Murray, Brian Blankespoor, Espen B. Prydz, and Hai-Anh H. Dang. Mapping the world population one building at a time. *arXiv preprint arXiv: Arxiv-1712.05839*, 2017.
- [99] Eric Tzeng, Judy Hoffman, Ning Zhang, Kate Saenko, and Trevor Darrell. Deep domain confusion: Maximizing for domain invariance. *arXiv preprint arXiv:1412.3474*, 2014.
- [100] Guido M van de Ven and Andreas S Tolias. Generative replay with feedback connections as a general strategy for continual learning. *arXiv preprint arXiv:1809.10635*, 2018.
- [101] Guido M van de Ven and Andreas S Tolias. Three scenarios for continual learning. *arXiv preprint arXiv:1904.07734*, 2019.
- [102] Hemanth Venkateswara, Jose Eusebio, Shayok Chakraborty, and Sethuraman Panchanathan. Deep hashing network for unsupervised domain adaptation. In *Proceedings of the IEEE conference on computer vision and pattern recognition*, pages 5018–5027, 2017.
- [103] Sherrie Wang, William Chen, Sang Michael Xie, George Azzari, and David B Lobell. Weakly supervised deep learning for segmentation of remote sensing imagery. *Remote Sensing*, 12(2): 207, 2020.
- [104] Minghao Xu, Jian Zhang, Bingbing Ni, Teng Li, Chengjie Wang, Qi Tian, and Wenjun Zhang. Adversarial domain adaptation with domain mixup. In *Proceedings of the AAAI Conference on Artificial Intelligence*, volume 34, pages 6502–6509, 2020.

- [105] Chaoqi Yang, Cao Xiao, Lucas Glass, and Jimeng Sun. Change matters: Medication change prediction with recurrent residual networks. *arXiv preprint arXiv:2105.01876*, 2021.
- [106] Huaxiu Yao, Long-Kai Huang, Linjun Zhang, Ying Wei, Li Tian, James Zou, Junzhou Huang, et al. Improving generalization in meta-learning via task augmentation. In *International Conference on Machine Learning*, pages 11887–11897. PMLR, 2021.
- [107] Huaxiu Yao, Ying Wei, Long-Kai Huang, Ding Xue, Junzhou Huang, and Zhenhui Jessie Li. Functionally regionalized knowledge transfer for low-resource drug discovery. *Advances in Neural Information Processing Systems*, 34, 2021.
- [108] Huaxiu Yao, Yu Wang, Sai Li, Linjun Zhang, Weixin Liang, James Zou, and Chelsea Finn. Improving out-of-distribution robustness via selective augmentation. In *ICML*, 2022.
- [109] Nanyang Ye, Kaican Li, Haoyue Bai, Runpeng Yu, Lanqing Hong, Fengwei Zhou, Zhenguo Li, and Jun Zhu. Ood-bench: Quantifying and understanding two dimensions of out-of-distribution generalization. In *Proceedings of the IEEE/CVF Conference on Computer Vision and Pattern Recognition*, pages 7947–7958, 2022.
- [110] Xiangyu Yue, Yang Zhang, Sicheng Zhao, Alberto Sangiovanni-Vincentelli, Kurt Keutzer, and Boqing Gong. Domain randomization and pyramid consistency: Simulation-to-real generalization without accessing target domain data. In *Proceedings of the IEEE/CVF International Conference on Computer Vision*, pages 2100–2110, 2019.
- [111] Friedemann Zenke, Ben Poole, and Surya Ganguli. Continual learning through synaptic intelligence. In *Proceedings of the 34th International Conference on Machine Learning-Volume 70*, pages 3987–3995. JMLR. org, 2017.
- [112] Hongyi Zhang, Moustapha Cisse, Yann N Dauphin, and David Lopez-Paz. mixup: Beyond empirical risk minimization. 2018.
- [113] Jingzhao Zhang, Aditya Menon, Andreas Veit, Srinadh Bhojanapalli, Sanjiv Kumar, and Suvrit Sra. Coping with label shift via distributionally robust optimisation. In *ICLR*, 2021.
- [114] Chunting Zhou, Xuezhe Ma, Paul Michel, and Graham Neubig. Examining and combating spurious features under distribution shift. In *ICML*, 2021.
- [115] Kaiyang Zhou, Yongxin Yang, Timothy Hospedales, and Tao Xiang. Deep domain-adversarial image generation for domain generalisation. In *Proceedings of the AAAI Conference on Artificial Intelligence*, volume 34, pages 13025–13032, 2020.

A Dataset Description

A.1 Yearbook

A.1.1 Setup

Problem Setting. The task is classifying the gender of an American high schooler from a yearbook photo. The input x is a 32×32 grayscale image, and the label y is male or female.

Data. Yearbook is based on the Portraits dataset [26] (MIT license), which collected and processed 37,921 frontal-facing yearbook portraits from 1905 – 2013 from 128 American high schools in 27 states. The Portraits dataset reflects changing fashion styles and social norms over the decades.

The original Portraits dataset did not evaluate models under a distribution shift setting. We use a subset of the Portraits dataset, consisting of data from 1930 – 2013. Our fixed time split (Eval-Fix) uses the first 41 years (1930 – 1970) for ID, and the remaining 43 years for OOD (1971 – 2013). For streaming evaluation (Eval-Stream), we treat each year as a single timestamp. For each timestamp, we randomly allocate 10% of the data to training, and the remaining 90% for validation. For OOD testing, all samples in each year are used. We provide the number of examples allocated to ID Train, ID Test, and OOD Test for each timestamp in Table 3.

The original Portraits dataset is provided as a set of hierarchical directories, organized by year, with PNG images of size 96×96 pixels. To reduce download times and I/O usage, we downsample the images from [26] to 32×32 pixels. We exclude the first 25 years (1905 – 1929) due to few samples in these years.

Table 3: Data subset sizes for the Yearbook task.

Years	ID Train	ID Test	OOD Test
1930 - 1934	1,051	120	1,171
1935 - 1939	1,361	154	1,515
1940 - 1944	2,047	230	2,277
1945 - 1949	1,979	222	2,201
1950 - 1954	1,604	181	1,785
1955 - 1959	1,820	205	2,025
1960 - 1964	1,482	167	1,649
1965 - 1969	2,812	315	3,127
1970 - 1974	2,326	260	2,586
1975 - 1979	2,329	261	2,590
1980 - 1984	2,654	298	2,952
1985 - 1989	2,239	251	2,490
1990 - 1994	2,207	249	2,456
1995 - 1999	2,564	287	2,851
2000 - 2004	2,447	274	2,721
2005 - 2009	1,407	159	1,566
2010 - 2013	1,102	125	1,227
Fixed-time split	14,901	1,677	21,439

Evaluation Metrics. We evaluate models by their average and worst-time OOD accuracies. The former measures the model’s ability to generalize across time, while the latter additionally measures model robustness to trends in time-specific visual patterns.

Eval-Stream evaluates performance across the next 10 years to test on visual trend changes over the decade without resulting in an unreasonably long evaluation time, due to the large number of timestamps in this dataset.

A.1.2 Broader Context

Facial recognition has been widely adopted in recent years. Employed by governments and private companies, facial recognition models are used in smartphones, robotics, advanced human-computer interaction systems. However, human appearance shifts over time due to changing social norms (e.g., the practice of smiling to the camera) and fashion trends (e.g., hair styles, popularity of eyewear). To remain reliable and effective, facial recognition models must be robust to changes in human appearance over time.

While Yearbook is not a facial recognition task, the Yearbook dataset can be used to train facial image analysis models that are robust to changes in appearance over time.

A.2 FMoW-Time

A.2.1 Setup

Problem Setting. The task in the FMoW-Time dataset is to classify the functional purpose of a region inside a satellite image. The input x is an 224×224 RGB satellite image, and the label y is one of 62 categories of building or land use. The data was collected from 16 different years. Our fixed time split (Eval-Fix) allocates the first 12 years for training and the last 4 years for testing. For streaming evaluation (Eval-Stream), we treat each year as a single timestamp.

Data. FMoW-Time is based on the Functional Map of the World dataset (license: <https://github.com/fMoW/dataset/blob/master/LICENSE>) [16], a dataset of satellite images taken from 2002 – 2018, from over 200 countries. Each satellite image is labeled according to the functional purpose of the buildings or land depicted in the image.

Table 4: Data subset sizes for the FMoW-Time task.

Year	ID Train	ID Test	OOD Test
2002	1,455	448	1,903
2003	1,985	570	2,555
2004	1,545	450	1,995
2005	2,207	629	2,836
2006	2,765	796	3,561
2007	1,338	349	1,687
2008	1,975	584	2,559
2009	6,454	1,920	8,374
2010	16,498	4,915	21,413
2011	19,237	5,711	24,948
2012	21,404	6,438	27,842
2013	3,465	385	3,850
2014	5,572	620	6,192
2015	8,885	988	9,873
2016	14,363	1,596	15,959
2017	5,534	615	6,149
Eval-Fix split	76,863	22,810	42,023

We adapt the version of the FMoW dataset from the WILDS benchmark [55], which consists of 141,696 RGB satellite images resized to 224×224 pixels. The train/val/test data splits in FMoW-WILDS contain images from disjoint location coordinates, and all splits contain data from all 5 geographic regions. For FMoW-Time, we partition each year’s data into train/validation as follows. For 2002 – 2013, we use the FMoW-WILDS Training (ID) split for training, and the Validation (ID) and Test (ID) splits for validation. For 2013 – 2015, we use data in the Validation (OOD) split and allocate 90% of the data from each year to train, and the remaining 10% to validation. For 2015 – 2017, we allocate 90% of the data from each year in the Test (OOD) split to train, and the remaining 10% to validation. Our fixed time split (Eval-Fix) uses the first 11 years (2002 – 2013) for training, and the remaining 5 years (2013 – 2018) for testing. For streaming evaluation (Eval-Stream), we treat each year as a single timestamp. We provide the number of examples allocated to ID Train, ID Test, and OOD Test at each timestamp in Table 4.

Evaluation Metrics. We evaluate models with the top-1 accuracy, both in terms of the average across all OOD timestamps and the accuracy on the worst timestamp. The former measures the model’s ability to reliably generalize across time and the latter more specifically tests the robustness at the most severe shifts. For Eval-Stream, we evaluate performance across the next 6 years.

A.2.2 Broader Context

ML models for satellite imagery can automate applications such as deforestation tracking, population density prediction, crop yield prediction [31, 98, 103]. Visual features in satellite data change over time due to both human and environmental activity, requiring a model that makes predictions for recent images using labeled data from the past. Through such applications, policy and humanitarian efforts would greatly benefit from temporally robust models which can reliably monitor global-scale satellite imagery even when conditions change over time.

A.3 MIMIC-IV

A.3.1 Setup

Problem Setting. The MIMIC-IV dataset contains two tasks: MIMIC-Readmission and MIMIC-Mortality. For both of these tasks, the input x is the concatenated ICD9 codes of diagnosis and treatment for a single patient.

- **MIMIC-Readmission:** the task is predicting hospital readmission for a patient. The label y is whether the patient was readmitted to the hospital within 15 days.
- **MIMIC-Mortality:** the task is predicting in-hospital mortality for each patient. The label y is whether the patient passed away during their hospital stay.

Table 5: Data subset sizes for the two MIMIC-IV tasks, MIMIC-Mortality and MIMIC-Readmission.

3-Year Block	ID Train	ID Test	OOD Test
2008 - 2010	60,851	15,215	76,066
2011 - 2013	55,714	13,930	69,644
2014 - 2016	53,932	13,485	67,417
2017 - 2019	45,990	11,500	57,490
Eval-Fix split	116,565	29,145	124,907

Data. The MIMIC-IV database [48] contains deidentified EHRs of 382,278 patients admitted to the emergency department or intensive care unit (ICU) at the Beth Israel Deaconess Medical Center (BIDMC) from 2008 – 2019. To protect patient privacy, the reported admission year is in a three year long date range. Hence, our timestamps are groups of three years: 2008 – –2010, 2011 – –2013, 2014 – –2016, 2017 – –2019. We considered ICU patient data sourced from the clinical information system MetaVision at the BIDMC, released in the MIMIC-IV v1.0 dataset, which contains 53,150 patient records. MIMIC-IV requires PhysioNet credentialing for use of human subject data.

We use a subset of the original MIMIC-IV dataset, where we regard each admission as one entry. For each admission, we collect the ICD9 codes of diagnosis and treatment. For each record, we concatenate the corresponding ICD9 codes [80] of diagnosis and treatment. We use the concatenated diagnosis and treatment ICD9 codes as the input feature. Our fixed time split (Eval-Fix) uses the first 6 years (2008 – 2013) for training, and the remaining 6 years for testing (2014 – 2019). For streaming evaluation (Eval-Stream), we treat each three-year block as a single timestamp. We allocate 20% of the data at each timestamp for test, and the rest for training. For OOD testing, all samples in each three-year block are used. We provide the number of examples allocated to ID Train, ID Test, and OOD Test for each timestamp in Table 5.

Evaluation Metrics. For MIMIC-Readmission, we evaluate models by their average and worst-time OOD accuracies. For MIMIC-Mortality, we evaluate models by their average and worst-time ROC-AUC due to label imbalance. The average metric measures the model’s ability to generalize across time, while the worst-time metric additionally measures model robustness to temporal distribution shifts in patient data. Eval-Stream evaluates performance across the next 3 years, which represents 25% of all timestamps in the entire dataset.

A.3.2 Broader Context

Many applications of machine learning to clinical healthcare have emerged in the last decade, such as predicting disease risk [70], medication changes [105], patient subtyping [5], in-hospital mortality [30], and length of hospital stay [20]. However, a key obstacle in deploying machine learning-based clinical decision support systems is distribution shift associated with changes in healthcare over time [30]. Existing domain generalization and unsupervised domain adaptation algorithms have been shown to produce less robust models compared to ERM in a variety of tasks (e.g., mortality, length of stay, sepsis, and invasive ventilation prediction) on the MIMIC-IV dataset [30], underscoring the need for better approaches.

The MIMIC-IV Mortality and Readmission tasks evaluate model robustness to temporal shifts in clinical medicine.

A.4 Huffpost

A.4.1 Setup

Problem Setting. The task is classifying the news category of an article from the headline. The input x is a news headline, and the label y is one of 11 news categories.

Data. Huffpost is based on the Kaggle News Category Dataset [76] (license: CC0: Public Domain), which contains approximately 200,000 news headlines and their corresponding news categories from the Huffington Post from 2012 – 2018. The Kaggle News Category Dataset contains 41 different news categories.

Table 6: Data subset sizes for the Huffpost task.

Year	ID Train	ID Test	OOD Test
2012	6,701	744	7,446
2013	7,492	832	8,325
2014	9,539	1,059	10,599
2015	11,826	1,313	13,140
2016	10,548	1,172	11,721
2017	7,907	878	8,786
2018	3,501	388	3,890
Eval-Fix split	35,558	3,948	24,397

We use a subset of the Huffpost dataset, consisting of 7 years from 2012 – 2018 and samples from 11 news categories (Black Voices, Business, Comedy, Crime, Entertainment, Impact, Queer Voices, Science, Sports, Tech, Travel). We partition the data by year.

Our fixed time split (Eval-Fix) uses 2016 as the time split, allocating 2012 – 2015 (4 years) for ID and 2016 – 2018 (3 years) for OOD. For streaming evaluation (Eval-Stream), we treat each year as a single timestamp. We allocate 10% of the data at each timestamp for test, and the rest for training. For OOD testing, all samples are used. Table 6 lists the number of examples allocated to ID Train, ID Test, and OOD Test for each timestamp.

The News Category Dataset is provided as a CSV file. We exclude news categories which do not appear in all years 2012 – 2018 to obtain the 11 news categories in Huffpost. We shuffle samples in each year, and randomly select 10% of the samples in each year as ID test and allocate the remaining 90% for training. For OOD testing, all samples in each year are used.

Evaluation Metrics. We evaluate models by their average and worst-time OOD accuracies. The former measures the model’s ability to generalize across time, while the latter additionally measures model robustness to trends in time-specific visual patterns.

Eval-Stream evaluates performance across the next 3 years, which represents 42.9% of the timestamps in the entire dataset.

A.4.2 Broader Context

Many language models which deal with information correlated with time exhibit performance degradation in downstream tasks such as Twitter hashtag classification [45] or question answering systems [66]. These performance drops along the temporal dimension reflect changes in the style or content of news that change over time. For instance, American politics in 2022 is more polarized than it was in 2012, according to a study by the Pew Research Center [19]. Models must be robust to such changes in factual knowledge.

A.5 arXiv

A.5.1 Setup

Problem Setting. The task is classifying the primary classification category of a research paper from the title. The input x is the paper title, and the label y is one of 172 paper categories.

Data. arXiv is based on the Kaggle arXiv Dataset [17] (license: CC0: Public Domain), which provides metadata of arXiv preprints from 2007 – 2023. These include: arXiv id, submitter, authors, title, comments, journal-ref, doi, abstract, categories, and versions.

We use a subset of the Kaggle arXiv dataset for arXiv, which consists of paper titles and their corresponding primary categories. Our fixed time split (Eval-Fix) uses 2016 as the time split, allocating data from 2007 – 2016 (10 years) for ID, and data from 2017 – 2022 (6 years) for OOD. For streaming evaluation (Eval-Stream), we treat each year as a single timestamp. We allocate 10% of the data at each timestamp for test, and the rest for training. For OOD testing, all samples are used. Table 7 lists the number of examples allocated to ID Train, ID Test, and OOD Test for each timestamp.

Table 7: Data subset sizes for the arXiv task.

Year	ID Train	ID Test	OOD Test
2007	131,550	14,616	146,167
2008	62,460	6,939	69,400
2009	206,244	22,916	229,161
2010	50,665	5,629	56,295
2011	55,741	6,193	61,935
2012	51,678	5,741	57,420
2013	64,951	7,216	72,168
2014	79,498	8,833	88,332
2015	193,979	21,553	215,533
2016	120,682	13,409	134,092
2017	111,024	12,336	123,361
2018	123,891	13,765	137,657
2019	142,767	15,862	158,630
2020	166,014	18,445	184,460
2021	201,241	22,360	223,602
2022	89,765	9,973	99,739
Eval-Fix split	1,017,448	113,045	927,449

The arXiv Dataset metadata is provided as a JSON file. We store only the primary category and the preprint title, and sort the data by update date, partitioning by year. We shuffle samples in each year, and randomly select 10% of the samples in each year as ID test and allocate the remaining 90% for training. For OOD testing, all samples in each year are used.

Evaluation Metrics. We evaluate models by their average and worst-time OOD accuracies. The former measures the model’s ability to generalize across time, while the latter additionally measures model robustness to trends in time-specific visual patterns.

Eval-Stream evaluates performance across the next 6 years, which represents 37.5% of all timestamps in the dataset.

A.5.2 Broader Context

Similar to changes in news and current events reflected in the Huffpost dataset, the content of arXiv preprints also change over time as research fields evolve. For example, “neural network attack” was originally a popular keyword in the security community, but it gradually became more prevalent in the machine learning community. As a result, primary categories of arXiv preprints shift over time.

B Algorithm Description

Before introducing all algorithms, we recall that each example is (x, y, t) , where x, y, t represent input feature, label, and timestamp, respectively.

B.1 Classical Supervised Learning

- **Empirical Risk Minimization (ERM).** We first consider Empirical Risk Minimization (ERM). This algorithm ignores the time information (t) and minimizes the average training loss

$$\theta^* = \arg \min_{\theta} \ell(x, y; f_{\theta}) \tag{3}$$

over the entire training dataset.

B.2 Continual Learning

- **Fine-tuning.** In fine-tuning, we use the newly observed labeled examples to continuously fine-tune the learned model without any explicit regularizer between consecutive timestamps.
- **Elastic Weight Consolidation (EWC).** Inspired by synaptic consolidation, EWC slows down the learning process for new tasks based on their relevance to previous tasks. Specifically, when

adapting to a new task, EWC’s loss function keeps the post-adaptation network parameters close to the parameters learned on previous tasks.

- **Synaptic Intelligence (SI)**. Motivated by synaptic dynamics, SI enables deep neural network to learn sequence of tasks by using synaptic state to track the parameter values and maintain online estimation of the importance of past learned experience.
- **Averaged Gradient Episodic Memory (A-GEM)**. Gradient Episodic Memory (GEM) leverages an episodic memory to store a selected set of examples from previous tasks in a continual learning setting. When adapting to a new task, the algorithm aims to make the updated model simultaneously perform well on examples in the new task and examples from the episode memory. A-GEM provides an efficient training strategy for Gradient Episodic Memory that significantly improves its computation and memory efficiency. Specifically, instead of making the updated model perform better on each individual previous tasks in the memory, A-GEM aims to produce a model that shows high average performance across the tasks in the episode memory.

B.3 Temporal Invariant Learning

- **CORAL**. CORAL penalizes the differences in the mean and covariance of the feature distributions of each domain. For CORAL, we adapted our implementation from the public repositories for DomainBed and WILDS [55]. CORAL is applicable to all datasets used in Wild-Time.
- **IRM**. Invariant risk minimization aims to learn an invariant predictor that performs well across all domains. The vanilla IRM objective can be reformulated as a bi-level optimization, which is challenging to solve. Following the original paper [3], we adopt IRM-v1 in this paper, an efficient approximation to the original IRM objective for learning invariant predictors.
- **Mixup** is an interpolation-based approach, which generates new training examples by applying the same interpolation strategies on the input features and their corresponding labels [112]. The original training samples are replaced by the newly generated samples for training.
- **LISA**. Motivated by mixup [112], LISA selectively interpolates examples to cancel out domain information. LISA has two variants — intra-label LISA and intra-domain LISA. Intra-label LISA interpolates examples with the same label but from different domains. Intra-domain LISA interpolates examples with the same domain but different labels. Furthermore, as mentioned in [108], intra-LISA performs better in domain shifts without considering domain information. We follow the implementation of Yao et al. [108] and only apply intra-label in Wild-Time.
- **GroupDRO**. GroupDRO uses distributionally robust optimization to optimize the worst-domain loss during the training stage. We follow the implementation of Sagawa et al. [88] and apply group adjustments, strong penalty and early stopping in GroupDRO.

B.4 Self-Supervised Learning

- **SimCLR** [15] is a simple contrastive learning approach for visual recognition. It uses normalized temperature-scaled cross entropy as the loss function and introduces a nonlinear transformation between the learned representation and the contrastive loss. We follow the implementation of Chen et al. [15].
- **SwAV** [11] simultaneously clusters the data and encourages the consistency of cluster assignments generated by different kinds of data augmentations. We follow the implementation of Caron et al. [11].

B.5 Bayesian Learning

- **SWA**. Stochastic Weight Averaging [41] averages multiple parameter values along the trajectory of SGD with almost no computational overhead. This method has been shown to lead to better in-distribution generalization due to its ability to find a better approximation to the posterior distribution over parameters. This property is reflected through the flatness of the learned optima. We follow the official implementation of SWA with the same learning rate as ERM and use default values for other hyperparameters.

C Experimental Details

All reported results are averaged over 3 random seeds. Experiments are conducted on a GPU-cluster with 6 GPU nodes. All classification tasks (i.e., Yearbook, FMoW-Time, MIMIC Mortality, MIMIC Readmission, Precipitation, HuffPost, arXiv) were trained with cross-entropy loss. In our experiments, we tune hyperparameters of all baselines by applying cross-validation with grid search.

For all methods, we use minibatch stochastic optimizers to train models, sampling uniformly from the ID set (in the Eval-Fix setting) or from each timestamp (in the Eval-Stream setting).

We report the number of train iterations used to train baselines for each dataset, under both the Eval-Fix and Eval-Stream settings. A single train iteration corresponds to one update via loss backpropagation. Under the Eval-Fix setting, the number of train iterations is the number of updates to the model on the ID train set. Under the Eval-Stream setting, in which models are trained incrementally, the number of train iterations corresponds to the number of updates to the model at each timestamp.

C.1 Eval-Fix Split Determination

To determine the time splits for the Eval-Fix setting of each dataset, we considered all ID/OOD splits ranging from 40%-60% ID/OOD to 80%-20% ID/OOD. For each of these time splits, we ran ERM on the ID and OOD sets, and selected the split with the largest discrepancy between average ID accuracy and average OOD accuracy.

C.2 Detailed Set Split Strategy

Suppose we have T timestamps. At each timestamp, we randomly sample 90% of the examples for training, and allocate the remaining 10% validation examples for ID evaluation. We detail the difference between the Eval-Fix and Eval-Stream setting as follows:

Eval-Fix Setting. In Eval-Fix, as shown in Figure 5, we have a split timestamp t_s . The ID timestamps are $t < t_s$, and the OOD timestamps are $t \geq t_s$. The training set consists of all training examples from the ID timestamps $t < t_s$. The ID validation set consists of all validation examples from the ID timestamps $t < t_s$. All examples in all test timestamps $t \geq t_s$ are used as the OOD test set.

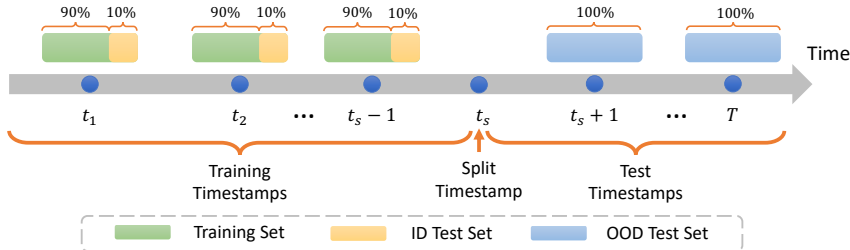


Figure 5: Data split under Eval-Fix setting.

Eval-Stream Setting. In Eval-Stream, at each evaluation timestamp, we evaluate across the next K timestamps. Specifically, at each timestamp $t \in [1, \dots, T]$, we evaluate our model across the timestamps $\{t + 1, \dots, t + K\}$, which is illustrated in Figure 6.

Hence, Eval-Fix can be viewed as a single timestamp evaluation within Eval-Stream, where we evaluate only at t_s and set $n = T - t_s$.

C.3 Hyperparameter Settings and Model Architectures

C.3.1 General Settings

Yearbook. We use a 4-layer convolutional network. Each convolutional layer has kernel size 3×3 , stride of 1×1 , padding of size 1, 32 output channels, a spatial batch norm layer, ReLU activation, and a 2D max pool layer with kernel size 2×2 .

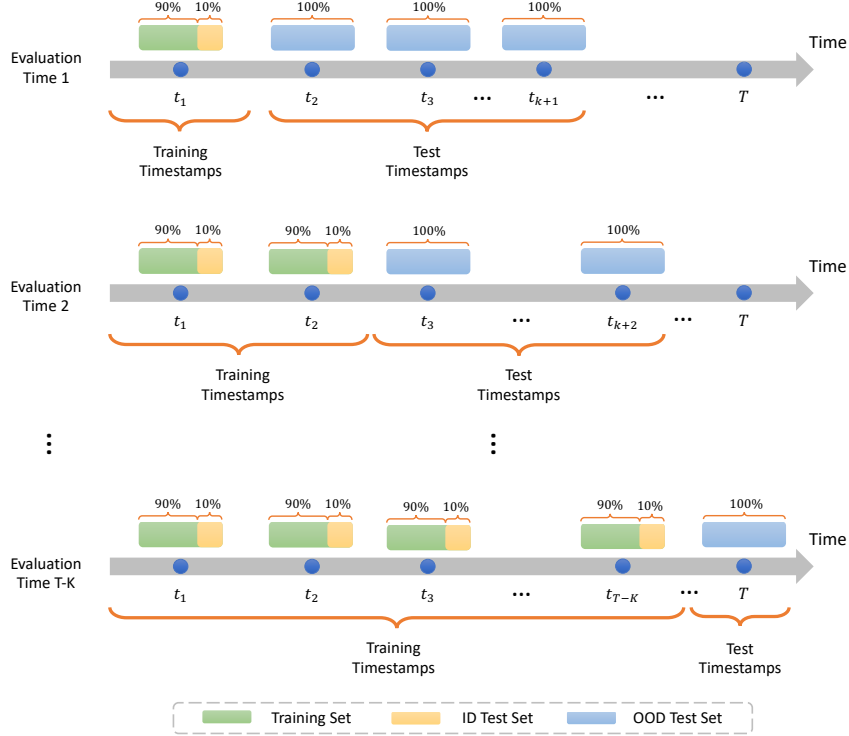


Figure 6: Data split under Eval-Stream setting.

We use the Adam optimizer with a fixed learning rate of 10^{-3} and train with a batch size of 32. Baselines were trained for 3000 iterations under the Eval-Fix setting and for 100 iterations under the Eval-Stream setting.

FMoW-Time. Following [55] and [16], we use a DenseNet-121 model [36] pretrained on ImageNet with no L_2 regularization.

We use the Adam optimizer with an initial learning rate of 10^{-4} that decays by 0.96 per epoch and a batch size of 64. Baselines were trained for 3000 iterations for the Eval-Fix setting and for 500 iterations for the Eval-Stream setting.

MIMIC-IV. We use a Transformer, consisting of an encoder and a decoder. Here, we collect the vocabulary based on the ICD9 codes.

We use the Adam optimizer with a learning rate of 5×10^{-4} and a batch size of 128. Baselines were trained for 3000 iterations under the Eval-Fix setting and for 500 iterations under the Eval-Stream setting.

Huffpost. We use a network backbone comprising of a pretrained DistilBERT base model (uncased) from [90] and a fully-connected, classification layer.

We use the AdamW optimizer with a learning rate of 2×10^{-5} , weight decay of 10^{-2} , and train with a batch size of 32. Baselines were trained for 6000 iterations under the Eval-Fix setting and for 1000 iterations under the Eval-Stream setting.

arXiv. We use the same network backbone, optimizer, learning rate, weight decay, and number of train iterations as those used for the Huffpost dataset. We train all baselines with a batch size of 64.

C.3.2 Algorithm-Specific Hyperparameters

Temporally Invariant Methods For GroupDRO, CORAL, and IRM, we follow WILDS [55] and use minibatch stochastic optimizers to train models, sampling uniformly from each substream (i.e., the domain in our temporal robustness setting), regardless of the number of training examples in the substream.

Table 8: Hyperparameters for CORAL, GroupDRO, and IRM baselines on all WildT datasets.

Dataset	CORAL Penalty	IRM Penalty	lr	# Substreams	Substream Size
Yearbook	0.9	1.0	1e-1	10	5
FMoW-Time	0.9	1.0	1e-4	3	3
MIMIC-IV-Mort	1.0	1.0	5e-4	4	3
MIMIC-IV-Readmit	1.0	1.0	5e-4	3	3
HuffPost	0.9	1.0	2e-5	3	2
arXiv	0.9	1.0	2e-5	4	4

- **GroupDRO.** We adapted the implementation of GroupDRO from Sagawa et al. [88] and Koh et al. [55]. Each example in the minibatch is sampled independently with uniform probabilities across substreams.

We list the hyperparameters used for GroupDRO on all WildT datasets in Table 8; namely, the number of substreams (e.g., number of groups) and substream size (e.g., group size).

- **CORAL.** We adapted the implementations of DeepCORAL from Gulrajani and Lopez-Paz [29] and Koh et al. [55], and compute CORAL penalties between features from all pairs of substreams, which we treat as groups/domains.

We list the hyperparameters used for CORAL on all WildT datasets in Table 8, which include the CORAL penalty λ_c , number of substreams (e.g., number of groups), and substream size (e.g., group size). CORAL was trained with a penalty of $\lambda_c = 0.1$ on the MIMIC-Mortality task, and $\lambda_c = 1.0$ on the MIMIC-Readmission task. For all remaining datasets, we used a default penalty of $\lambda_c = 0.9$.

- **IRM.** We adapted the implementations of IRM from Arjovsky et al. [3] and Koh et al. [55]. We list the hyperparameters used for IRM on all WildT datasets in Table 8, which include the IRM penalty λ_i , number of substreams (e.g., number of groups), and substream size (e.g., group size). IRM was trained with a penalty of $\lambda_i = 1.0$ on all datasets.
- **LISA.** We adapted the implementation of LISA from Yao et al. [108] and implemented intra-label LISA, where training samples with the same label are interpolated. For the Yearbook and FMoW-Time datasets, the input image tensors were interpolated. For the arXiv, Huffpost, and MIMIC-IV datasets, the learned feature representations were interpolated.

All LISA experiments were conducted with $\alpha = 2.0$, where the interpolation ratio $\lambda \in [0, 1]$ is drawn from a Beta(α, α) distribution.

- **Mixup.** For mixup, we use the same hyperparameters as ERM.

Continual Learning Methods

- **A-GEM.** We adapted the implementation of A-GEM from Chaudhry et al. [14] and "Mammoth - An Extendible (General) Continual Learning Framework for Pytorch" [7, 9]. All A-GEM experiments were conducted with a default buffer size of 1000.
- **EWC.** We adapted the implementation of EWC from Kirkpatrick et al. [54], van de Ven and Tolias [100], and van de Ven and Tolias [101]. For the EWC loss regularization strength, we use a default value of 0.5 for the Yearbook, FMoW-Time, Huffpost, arXiv, and MIMIC-IV-Readmit datasets. For MIMIC-IV-Mortality, we use 1.0.
- **SI.** We adapted the implementation of SI from Zenke et al. [111], van de Ven and Tolias [100], van de Ven and Tolias [101]. For the SI loss regularization strength λ_s , we use a default value of 0.1 for all datasets.

Self-Supervised Methods

- **SimCLR.** We implement SimCLR using the Lightly framework [40]. We apply SimCLR to learn representations, and then fine-tune the model with the same (labeled) training data. For both Yearbook and FMoW-Time, we use the set of image transforms from Chen et al. [15]. Specifically, we sequentially apply the following three random augmentations: random cropping followed by resize back to the original size, color distortions, and Gaussian blur. We list all hyperparameters in Table 9.

Table 9: Hyperparameters for SimCLR on Yearbook and FMoW-Time.

Dataset	Yearbook	FMoW-Time
Prob. Color Jitter	0.8	0.8
Color Jitter Strength	0.5	0.5
Min. Crop Scale	0.08	0.08
Prob. Grayscale	0.2	0.2
Kernel Size	0.1×32	0.1×224
Prob. Vertical Flip	0.5	0
Prob. Horizontal Flip	0.5	0.5
Prob. Rotation (+90)	0.0	0.5
Embedding Dim.	128	128
No. SSL Iters.	2700	1500
No. Finetune Iters.	300	1500

Table 10: Hyperparameters for SwaV on Yearbook and FMoW-Time.

Dataset	Yearbook	FMoW-Time
No. Views	2	2
Crop Sizes	224, 96	224, 96
No. Crops	2, 6	2, 6
Min. Crop Scale	0.08, 0.05	0.08, 0.05
Max. Crop Scale	1.0, 0.14	1.0, 0.14
Prob. Horizontal Flip	0.5	0.5
Prob. Color Jitter	0.8	0.8
Color Jitter Strength	0.8	0.8
Prob. Grayscale	0.2	0.2
Embedding Dim.	128	128
No. Prototypes	32	1024
No. SSL Iters.	2700	1500
No. Finetune Iters.	300	1500

Table 11: Hyperparameters for EWC and SI baselines on all WildT datasets.

Dataset	EWC λ_e	SI λ_s
Yearbook	0.5	0.1
FMoW-Time	0.5	0.1
MIMIC-IV-Mort	1.0	0.1
MIMIC-IV-Readmit	0.5	0.1
HuffPost	0.5	0.1
arXiv	0.5	0.1

- **SwaV.** We implement SwaV using the Lightly framework [40]. We apply SwaV to learn representations, and then fine-tune the model with the same training data. We follow the multi-crop augmentation strategy proposed by Caron et al. [11]. We use 2 views and list all hyperparameters in Table 10.

Bayesian Methods

- **SWA.** We follow the official implementation of SWA [41, 4]. We use the same learning rate as ERM and use default values for other hyperparameters.

D Results Under Eval-Stream Setting

Under Eval-Stream setting, we visualize the average performance and worst-time performance for every timestamp. For each timestamp, we calculate the average/worst performance over the evaluated time window. The results of all tasks are shown in Figure 7. The key observations are very close to the findings under Eval-Fix setting. Additionally, invariant learning approaches performs slightly better than continual learning approaches in most tasks.

Under the Eval-Stream setting, we further explain why continual learning approaches fail to improve over other baselines in the Eval-Stream setting from the following two reasons: (1) Most existing continual learning approaches focus on backward transfer (i.e., catastrophic forgetting). In Wild-Time, we focus on forward transfer, and evaluate performance on future timestamps (i.e., temporal robustness); (2) For continual learning approaches that also focus on forward transfer (e.g., A-GEM), most of these approaches only show improvements on manually delineated sets of tasks with artificial temporal variations (e.g., Split CUB, Split CIFAR), but are not evaluated on benchmarks with natural temporal distribution shifts, such as Wild-Time. Analogously, we note that invariant learning approaches show improvements in artificial datasets (e.g., ColoredMNIST, Waterbirds [88]), but fail to outperform ERM in benchmarks with natural distribution shifts, e.g., WILDS [55].

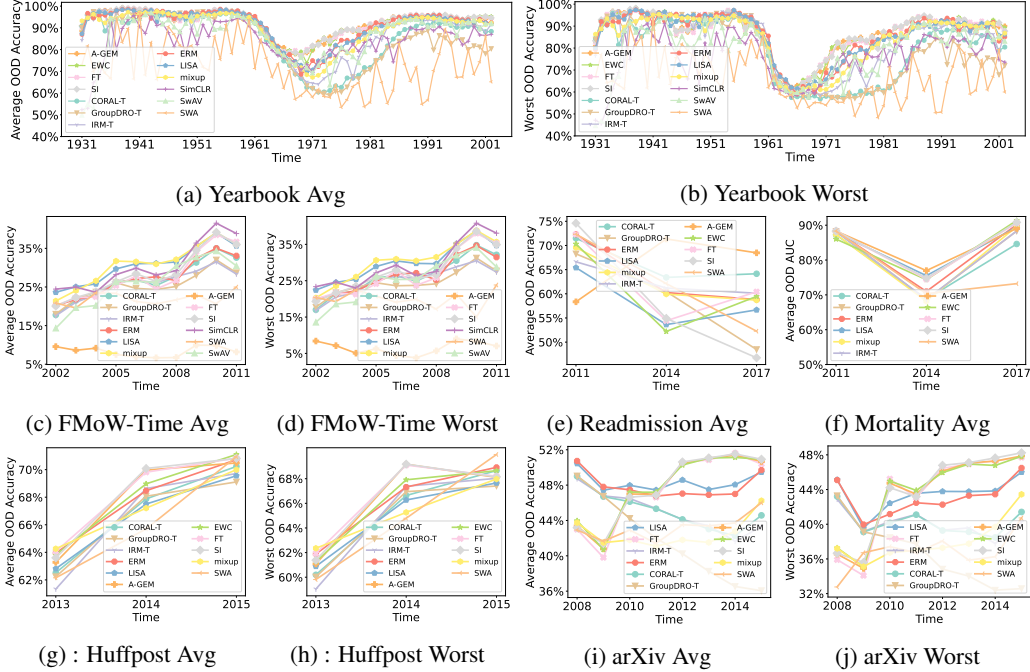


Figure 7: Results under Eval-Stream Setting. Note that for MIMIC-Readmission (e) and MIMIC-Mortality (f), we only report the average timestamp performance as we only evaluate on the next timestamp, which is a three-year block.

E Additional Experiments under Eval-Fix Setting

E.1 Standard Split vs. Mixed Split

We verify that the performance gap between ID and OOD timestamps are not caused by the difficulty of examples from OOD timestamps. First, we analyze the effect of the difficulty of OOD examples. We use two kinds of data splits – standard split and mixed split. In the standard split, the model is trained on timestamps before the split time and then evaluated on examples from future timestamps. In the mixed split, the training data is merged from all timestamps, and the model is evaluated on the original OOD examples. We report the results in Table 12 and observe large performance gaps between standard split and mixed split on all Wild-Time tasks. The observation verifies that the performance gaps between ID and OOD are not caused by the difficulty.

For each Wild-Time dataset, we plot the label distributions over time in Figure 8. We observe that the label distributions change over time for all Wild-Time datasets, as this is a naturally-occurring shift that we aim to tackle with the Wild-Time benchmark.

Table 12: Performance drops of ERM with different splits under Eval-Fix setting. In the standard split, we train the model on timestamps before the split timestamp, and evaluate the model in the future timestamps. In the mixed split, we merge the training data from all timestamps, and evaluate the model on the original OOD set. The large gap between standard split and mixed split indicates that the performance drops between ID and OOD shown in Table 1 in the main paper are not caused by the difficulty of the examples from OOD timestamps.

Dataset	Standard Split		Mixed Split	
	OOD Avg.	OOD Worst	OOD Avg.	OOD Worst
Yearbook	81.98%	69.62%	94.57%	78.57%
FMoW-Time	54.07%	46.00%	57.80%	52.00%
MIMIC-Mortality	72.89%	65.80%	91.00%	88.67%
MIMIC-Readmission	61.33%	59.46%	57.18%	54.84%
Huffpost	70.42%	68.71%	78.11%	76.87%
arXiv	45.94%	44.09%	52.12%	50.57%

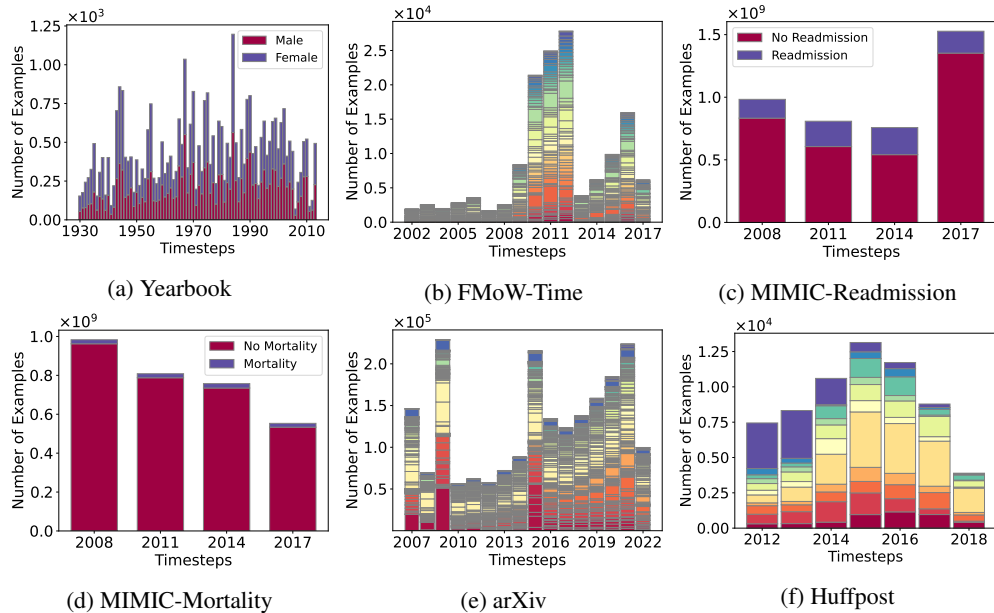


Figure 8: Label distributions of all Wild-Time classification datasets over time. Note that we include legends for datasets with less than 8 classes due to space limitations.

E.2 Temporal Adaptation of Invariant Learning Methods

In this section, we provide additional analysis for temporal adaptation, including the analysis of the effectiveness of temporal adaptation, the effect of time window size, and the comparison between overlapping and non-overlapping substreams.

E.2.1 Temporal Adaptation Improves Performance

We compare the temporal adapted invariant learning approaches with the original approaches. The results are listed in Table 13. We observe that temporal adaptation indeed shows improved performance over vanilla invariant learning approaches, verifying the efficacy of the proposed strategy.

E.2.2 Effect of Time Window Size

We include an ablation in which we report the performance of CORAL-T, GroupDRO-T, and IRM-T when the time window size L (defined in Section 4 of the main paper) is reduced. We report baseline results in Table 14. We found that reducing L marginally worsens the performance of invariant learning baselines.

E.2.3 Non-Overlapping Time Windows

In the proposed temporal adaptations of the invariant learning methods (CORAL-T, GroupDRO-T, IRM-T), we use overlapping time windows to capture the gradual temporal distribution shift. Here, we run all invariant learning baselines using non-overlapping windows, and report the OOD performance in Table 15. For the Yearbook, Huffpost, arXiv, MIMIC-Mortality, and MIMIC-Readmission, invariant learning baselines generally obtained better performance using overlapping time windows. Since, on the aggregate, using overlapping time windows resulted in better performance, we keep the results using non-overlapping windows in Table 2 of the main paper.

E.3 Effect of Model Backbones

We investigate the effect of different models backbones on a Wild-Time image dataset (FMoW-Time) and text dataset (arXiv). Specifically, we use ResNet18 and ResNet50 backbones for FMoW-Time, and BERT and ALBERT backbones for arXiv. We report the performance of ERM and two

Table 13: The vanilla versus temporal adapted invariant learning performance of each method evaluated on Wild-Time under the Eval-Fix setting.

	Yearbook (Accuracy (%) \uparrow)		FMoW-Time (Accuracy (%) \uparrow)		MIMIC-Readmission (Accuracy (%) \uparrow)	
	OOD Avg.	OOD Worst	OOD Avg.	OOD Worst	OOD Avg.	OOD Worst
GroupDRO	76.19 (1.58)	59.61 (1.09)	42.54 (0.39)	35.17 (1.08)	55.69 (3.53)	54.18 (2.79)
GroupDRO-T	77.06 (1.67)	60.96 (1.83)	43.87 (0.55)	36.60 (1.25)	56.12 (4.35)	53.12 (4.41)
CORAL	76.29 (1.75)	58.54 (2.91)	48.96 (0.23)	40.17 (0.89)	56.62 (3.21)	54.08 (3.50)
CORAL-T	77.53 (2.15)	59.34 (1.46)	49.43 (0.38)	41.23 (0.78)	57.31 (4.45)	54.69 (4.36)
IRM	77.08 (2.05)	63.79 (1.27)	45.25 (1.01)	38.73 (0.69)	57.89 (2.76)	53.02 (2.53)
IRM-T	80.46 (3.53)	64.42 (4.38)	45.00 (1.18)	37.67 (1.17)	56.53 (3.36)	52.67 (5.17)
	MIMIC-Mortality (AUC (%) \uparrow)		HuffPost (Accuracy (%) \uparrow)		arXiv (Accuracy (%) \uparrow)	
	OOD Avg.	OOD Worst	OOD Avg.	OOD Worst	OOD Avg.	OOD Worst
GroupDRO	74.93 (3.17)	70.58 (3.46)	68.33 (0.88)	67.42 (1.27)	37.37 (1.09)	36.09 (0.93)
GroupDRO-T	76.88 (4.74)	71.40 (6.84)	69.53 (0.54)	67.68 (0.78)	39.06 (0.54)	37.18 (0.52)
CORAL	76.83 (2.70)	64.62 (5.58)	70.64 (0.43)	67.82 (1.16)	40.82 (1.16)	38.16 (0.62)
CORAL-T	77.98 (2.57)	64.81 (10.8)	70.05 (0.63)	68.39 (0.88)	42.32 (0.60)	40.31 (0.61)
IRM	76.25 (5.87)	69.91 (6.02)	71.69 (1.33)	69.49 (1.46)	35.07 (0.55)	34.22 (0.63)
IRM-T	76.16 (6.32)	70.64 (8.99)	70.21 (1.05)	68.71 (1.13)	35.75 (0.90)	33.91 (1.09)

Table 14: Performance of the temporally adapted invariant learning baselines when decreasing the length of the time windows, L . We evaluate under the Eval-Fix setting and report the average and standard deviation (value in parentheses), computed over three random seeds. For Yearbook, performance worsens when L is reduced, but improves for FMoW-Time.

	L	Yearbook (Accuracy (%) \uparrow)		L	FMoW-Time (Accuracy (%) \uparrow)	
		OOD Avg.	OOD Worst		OOD Avg.	OOD Worst
GroupDRO-T	5	77.06 (1.67)	60.96 (1.83)	3	43.87 (0.55)	36.60 (1.25)
	4	72.84 (3.04)	56.05 (0.75)	2	45.17 (0.83)	36.97 (1.00)
	2	73.42 (2.29)	56.99 (2.54)	n/a	n/a	n/a
CORAL-T	5	77.53 (2.15)	59.34 (1.46)	3	49.43 (0.38)	41.23 (0.78)
	4	77.09 (1.56)	59.17 (1.89)	2	49.67 (0.49)	41.63 (0.32)
	2	76.92 (1.07)	59.26 (1.38)	n/a	n/a	n/a
IRM-T	5	80.46 (3.53)	64.42 (4.38)	3	45.00 (1.18)	37.67 (1.17)
	4	79.56 (3.12)	63.70 (3.85)	2	48.50 (0.10)	40.63 (0.59)
	2	79.47 (2.69)	63.65 (3.91)	n/a	n/a	n/a

representative invariant learning and continual learning approaches – LISA and Fine-tuning – under the Eval-Fix setting in Table 16.

These results are consistent with our findings that neither invariant learning nor continual learning approaches make models more robust to temporal distribution shift, even with different backbones.

E.4 Reducing the Number of Training Examples

We analyze the performance of all baselines when reducing the number of training examples. Specifically, under the Eval-Fix setting, we randomly allocate 30% of the data at each training timestamp as training, rather than 90% in our original results (c.f., Table 2 in the main paper). We report all results in Table 17. We observe that ERM still outperforms invariant learning and continual learning approaches, corroborating our findings in the main paper.

Table 15: Performance of CORAL-T, GroupDRO-T, and IRM-T baselines when trained on non-overlapping time substreams. OL: Overlapping; NOL: Non-overlapping

		Yearbook (Accuracy (%) \uparrow)		FMoW-Time (Accuracy (%) \uparrow)		MIMIC-Readmission (Accuracy (%) \uparrow)	
		OOD Avg.	OOD Worst	OOD Avg.	OOD Worst	OOD Avg.	OOD Worst
CORAL-T	OL	77.53 (2.15)	59.34 (1.46)	49.43 (0.38)	41.23 (0.78)	57.31 (4.45)	54.69 (4.36)
	NOL	75.97 (0.63)	57.47 (0.29)	49.93 (0.64)	42.13 (0.96)	54.86 (2.93)	51.44 (4.63)
GroupDRO-T	OL	77.06 (1.67)	60.96 (1.83)	43.87 (0.55)	36.60 (1.25)	56.12 (4.35)	53.12 (4.41)
	NOL	76.94 (1.87)	58.58 (1.82)	48.67 (0.57)	45.50 (0.62)	53.96 (3.03)	50.47 (4.43)
IRM-T	OL	80.46 (3.53)	64.42 (4.38)	45.00 (1.18)	37.67 (1.17)	56.53 (3.36)	52.67 (5.17)
	NOL	77.21 (2.34)	59.44 (1.72)	49.67 (0.40)	42.50 (1.08)	54.31 (3.67)	51.08 (5.23)
		MIMIC-Mortality (AUC (%) \uparrow)		HuffPost (Accuracy (%) \uparrow)		arXiv (Accuracy (%) \uparrow)	
		OOD Avg.	OOD Worst	OOD Avg.	OOD Worst	OOD Avg.	OOD Worst
CORAL-T	OL	77.98 (2.57)	64.81 (10.8)	70.05 (0.63)	68.39 (0.88)	42.32 (0.60)	40.31 (0.61)
	NOL	71.57 (11.7)	65.77 (15.3)	68.11 (1.40)	66.94 (1.50)	42.07 (0.72)	40.10 (0.72)
GroupDRO-T	OL	76.88 (4.74)	71.40 (6.84)	69.53 (0.54)	67.68 (0.78)	39.06 (0.54)	37.18 (0.52)
	NOL	72.78 (10.7)	67.40 (14.1)	68.41 (0.41)	67.26 (0.49)	36.07 (1.35)	33.98 (1.46)
IRM-T	OL	76.17 (6.32)	70.64 (8.99)	70.21 (1.05)	68.71 (1.13)	35.75 (0.90)	33.91 (1.09)
	NOL	73.08 (9.99)	67.69 (13.1)	69.58 (0.79)	68.16 (0.64)	38.85 (0.44)	36.86 (0.42)

Table 16: Performance comparison w.r.t. Different backbones.

	Backbone	ERM	Fine-tuning	LISA
FMoW-Time	ResNet18	47.95 (0.39)	40.95 (0.50)	47.59 (0.36)
	ResNet50	52.91 (0.46)	45.68 (0.79)	53.17 (0.85)
	DenseNet101	54.07 (0.25)	44.22 (0.56)	52.33 (0.42)
arXiv	DistilBERT	45.94 (0.97)	50.31 (0.39)	47.82 (0.47)
	BERT	47.51 (1.20)	50.99 (0.52)	49.05 (1.01)
	ALBERT	45.25 (0.65)	49.76 (0.69)	46.01 (0.52)

F Datasets without Gradual Temporal Distribution Shifts

In this section, we discuss two additional datasets that were not included in Wild-Time. These datasets do not satisfy the criteria discussed in Section 2.1.

F.1 Drug-BA

F.1.1 Dataset Setup

Problem Setting. The task is predicting the binding affinity of candidate drugs to their target molecules. The input x contains molecular information of both the drug and target molecules, and the label y is the binding affinity value.

Data. The Therapeutics Data Commons (TDC) benchmark (MIT license). TDC offers the BindingDB dataset, which was curated from BindingDB, a public database that features drug-target binding affinities collected from a variety of sources, including patents, journals, and assays. Each entry in BindingDB consists of a small molecule and the corresponding target protein. We exclude data from the year 2021 in the original TDC benchmark as 2021 includes only one month’s worth of data.

For Eval-Fix, we use the first 4 years (2013 – 2016) for training and allocate 4 years (2017 – 2020) for testing. For streaming evaluation (Eval-Stream), we treat each year as a single timestamp. We provide the number of examples allocated to ID Train, ID Test, and OOD Test for each timestamp in Table 18.

Evaluation Metrics. We use Pearson Correlation Coefficient (PCC), which measures the amount of linear correlations between the true values and the predicted values, to evaluate model performance

Table 17: Performance of all baselines when reducing the amount of training data. We randomly allocate 30% of the data at each timestamp to training, rather than 90% in our original benchmark.

	Yearbook (Accuracy (%) \uparrow)			FMoW-Time (Accuracy (%) \uparrow)		
	ID Avg.	OOD Avg.	OOD Worst	ID Avg.	OOD Avg.	OOD Worst
Fine-tuning	46.29 (1.17)	52.00 (5.00)	44.10 (2.15)	40.30 (0.14)	39.34 (0.57)	30.91 (0.29)
EWC	45.50 (0.00)	48.84 (0.01)	42.86 (0.01)	40.89 (0.66)	39.99 (0.66)	31.24 (0.43)
SI	49.42 (6.73)	47.03 (17.2)	45.52 (4.61)	41.03 (0.19)	39.65 (0.53)	30.91 (0.29)
A-GEM	45.50 (0.00)	46.98 (3.57)	44.95 (3.45)	40.52 (0.56)	39.60 (0.41)	31.05 (0.38)
ERM	93.96 (1.72)	77.05 (5.13)	60.72 (2.92)	51.74 (0.77)	50.63 (0.56)	40.29 (0.94)
GroupDRO-T	77.56 (11.5)	60.45 (7.10)	47.03 (7.99)	40.16 (0.68)	39.52 (0.86)	31.62 (0.29)
mixup	92.88 (2.35)	77.31 (2.60)	61.56 (3.00)	54.23 (0.26)	53.77 (0.23)	43.04 (0.77)
LISA	92.51 (4.03)	74.17 (5.22)	57.39 (1.77)	51.34 (0.14)	50.76 (0.83)	40.12 (1.42)
CORAL-T	75.35 (19.7)	59.66 (10.1)	44.00 (10.58)	44.15 (0.93)	43.85 (0.46)	34.59 (0.25)
IRM-T	77.04 (17.7)	60.45 (7.10)	47.03 (7.99)	45.19 (0.94)	44.11 (1.23)	36.26 (1.36)
	MIMIC-Readmission (Accuracy (%) \uparrow)			MIMIC-Mortality (AUC (%) \uparrow)		
	ID Avg.	OOD Avg.	OOD Worst	ID Avg.	OOD Avg.	OOD Worst
Fine-tuning	74.22 (2.96)	64.20 (3.73)	62.33 (5.25)	87.92 (0.92)	59.20 (0.71)	50.00 (1.35)
EWC	74.49 (1.41)	66.75 (0.99)	65.93 (1.26)	87.94 (0.08)	60.07 (2.45)	51.21 (3.11)
SI	74.22 (2.96)	64.20 (3.73)	62.33 (5.25)	87.92 (0.92)	59.20 (0.71)	50.00 (1.35)
A-GEM	80.58 (0.14)	69.90 (0.01)	68.48 (0.01)	70.27 (17.5)	53.68 (3.76)	48.00 (1.83)
ERM	70.49 (2.47)	55.28 (2.54)	51.69 (5.47)	89.53 (0.82)	71.06 (7.63)	65.76 (10.2)
GroupDRO-T	74.36 (2.65)	59.90 (15.3)	54.92 (21.3)	89.48 (0.85)	73.28 (7.58)	68.25 (9.97)
mixup	71.82 (3.61)	41.57 (1.12)	30.29 (0.00)	89.48 (1.14)	71.32 (8.55)	65.65 (11.4)
LISA	67.50 (2.22)	40.48 (0.68)	30.29 (0.00)	90.01 (0.32)	73.37 (10.5)	68.97 (14.5)
CORAL-T	74.48 (1.72)	45.00 (4.50)	34.58 (7.05)	89.12 (1.43)	71.55 (10.4)	66.01 (13.6)
IRM-T	74.36 (1.90)	52.00 (14.4)	44.24 (20.0)	88.24 (1.59)	73.13 (10.1)	68.66 (13.5)
	HuffPost (Accuracy (%) \uparrow)			arXiv (Accuracy (%) \uparrow)		
	ID Avg.	OOD Avg.	OOD Worst	ID Avg.	OOD Avg.	OOD Worst
Fine-tuning	13.11 (1.03)	14.12 (3.27)	12.89 (2.46)	50.34 (0.13)	48.88 (0.26)	46.72 (0.25)
EWC	13.26 (1.27)	13.65 (1.51)	12.37 (1.03)	50.31 (0.17)	48.56 (0.05)	46.38 (0.11)
SI	13.06 (1.05)	14.22 (3.26)	12.95 (2.44)	50.35 (0.13)	48.88 (0.25)	46.72 (0.26)
A-GEM	13.07 (0.69)	15.53 (2.18)	13.43 (2.03)	50.36 (0.18)	48.79 (0.32)	46.53 (0.39)
ERM	15.86 (1.45)	12.32 (2.64)	11.32 (2.08)	53.55 (0.21)	46.07 (0.53)	44.16 (0.50)
GroupDRO-T	14.23 (1.05)	11.82 (1.07)	11.03 (0.76)	50.01 (0.03)	39.71 (0.63)	37.79 (0.65)
mixup	15.49 (0.92)	13.35 (1.45)	11.92 (1.08)	52.66 (0.13)	45.98 (0.47)	44.00 (0.45)
LISA	14.95 (0.68)	13.26 (3.62)	11.93 (2.54)	49.17 (0.43)	47.66 (0.27)	45.71 (0.30)
CORAL-T	16.56 (0.56)	13.15 (5.17)	11.82 (4.29)	52.60 (0.06)	42.72 (0.27)	40.72 (0.24)
IRM-T	14.06 (0.65)	11.39 (0.41)	11.05 (0.47)	46.20 (0.12)	35.85 (0.70)	34.14 (0.75)

in predicting drug-target binding affinity. Eval-Stream evaluates performance across the next 3 years, which represents 37.5% of all timestamps in the entire dataset.

F.1.2 Baseline Results and Analysis

Experimental Setup. We use the DeepDTA model from [81], which achieves state-of-the-art performance on drug target binding affinity prediction by using CNNs to construct high-level representations of a drug and a target. We use the Adam optimizer with a learning rate of 2×10^{-5} or 5×10^{-5} (for different baselines) and batch size of 256. Baselines were trained for 5000 iterations under the Eval-Fix setting and for 500 iterations under the Eval-Stream setting. In terms of hyperparameters for CORAL, GroupDRO and IRM, the CORAL penalty, IRM penalty, learning rate, the number of substreams and the size of substreams are set as 0.9, 10^{-3} , 5×10^{-5} , 3, 2, respectively. Notice that LISA is only applicable to classification problem, thus we do not evaluate LISA on Drug-BA.

Results. In Drug-BA, similar to Table 12, we reported the results of standard splits and mixed splits and the results of Eval-Stream and Eval-Fix in Figure 9. First, though the performance comparison between standard split and mixed split in the top table of Figure 9, we observe a significant drop between them, where OOD average performance drops from 0.724 (mixed split) to 0.357 (standard split). Second, the performance per test time in Figure 9(b) further indicates such

Table 18: Data subset sizes for the Drug-BA task.

Year	ID Train	ID Test	OOD Test
2013	9,121	2,281	11,402
2014	16,148	4,038	20,186
2015	24,251	6,063	30,314
2016	23,095	5,774	28,869
2017	41,203	10,301	51,504
2018	32,924	8,231	41,155
2019	33,607	8,402	42,009
2020	5,557	1,390	6,947
Eval-Fix split	72,615	18,156	141,615

Dataset	Standard Split		Mixed Split	
	OOD Avg.	OOD Worst	OOD Avg.	OOD Worst
Drug-BA	0.357	0.244	0.724	0.710

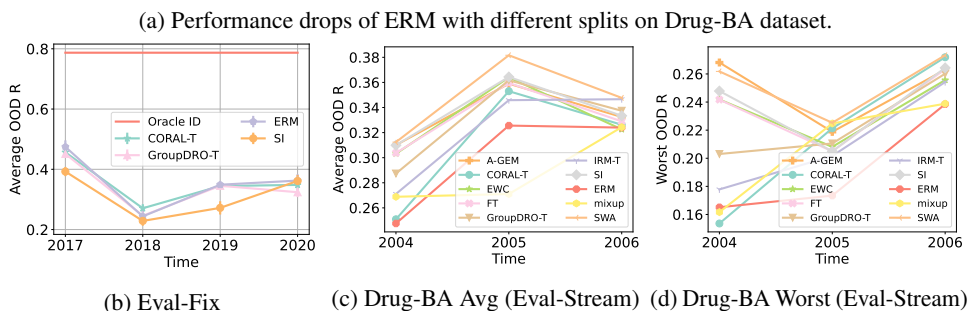


Figure 9: Results on Drug-BA. (b) out-of-distribution performance per test timestamp under Eval-Fix setting; (b) (c): results under Eval-Stream setting.

a sudden performance drop between Oracle ID and ERM in 2017. These results suggest that the Drug-BA dataset violates our criterion about gradual temporal distribution shifts. Thus, we exclude it in the official Wild-Time benchmark.

F.1.3 Broader Context

Drug discovery brings new candidate medications to potentially billions of people, allowing people to live longer and healthier lives. Traditional methods of drug discovery are via high-throughput, wet-lab experiments [38], which are expensive, time-consuming, and limited in their ability to search over large sets of drug candidates. Virtual screening is a computational pre-screening process in which the binding activity of a drug candidate with the target protein of a disease is predicted [12, 97]. Recently, there has been a surge of interest in applying machine learning to virtual screening, which can reduce costs and increase the search space to avoid missing potential drug candidates. Recent binding activity prediction models investigate binding pairs between existing compounds and target proteins [73, 81, 106, 107]. In practice, new target proteins or new classes of compounds appear over time, requiring machine learning models that are robust to subtle domain shifts across time.

F.2 Precipitation

F.2.1 Dataset Setup

Problem Setting. The task is classifying the precipitation level of a region. The input x is tabular data consisting of 123 meteorological features (1 categorical feature and 122 continuous features). The label y is one of 9 precipitation classes.

Data. Precipitation is based on the Shifts Precipitation Prediction dataset [72] (Apache-2.0 license), which collected and processed tabular Precipitation data from the Yandex Precipitation Service to provide a domain shift benchmark for two tasks: temperature prediction (scalar regression) and

Table 19: Data subset sizes for the Precipitation task.

Month	ID Train	ID Test	OOD Test
Sep 2018	698,134	77,570	775,705
Oct 2018	714,265	79,362	793,628
Nov 2018	613,885	68,209	682,095
Dec 2019	707,274	78,586	785,861
Jan 2019	739,325	82,147	821,473
Feb 2019	665,745	73,971	739,717
Mar 2019	729,527	81,058	810,586
Apr 2019	691,366	76,818	768,185
May 2019	673,058	74,784	747,843
Jun 2019	548,793	60,976	609,770
Jul 2019	680,152	75,572	755,725
Aug 2019	681,035	75,670	756,706
Eval-Fix split	4,868,155	540,903	3,638,229

precipitation classification (multi-class classification). The Shifts Precipitation Prediction dataset contains 10 million 129-column entries, consisting of 123 heterogeneous meteorological features, 4 meta-data attributes (e.g., time, latitude, longitude, and climate type), and 2 targets (temperature and precipitation class). The data is distributed uniformly between September 1, 2018 to September 1, 2019 and is partitioned by both time and climate type.

We use a subset of the original Shifts Precipitation Prediction dataset, using measurements taken from October 2018 - August 2019. The Precipitation dataset consists of 123 heterogeneous meteorological features, 1 target (precipitation class), and 1 metadata attribute (time). We partition the dataset by month. Our fixed time split (Eval-Fix) uses data from October 2018 - April 2019 (7 months) for ID, and data from May 2019 - August 2019 (4 months) for OOD. For streaming evaluation (Eval-Stream), we treat each month as a single timestamp. We allocate 10% of the data at each timestamp for test, and the rest for training. For OOD testing, all samples are used. Table 19 lists the number of examples allocated to ID Train, ID Test, and OOD Test for each timestamp.

The Shifts Precipitation Prediction dataset is provided as a CSV file. We ignore the latitude, longitude, and climate type metadata and filter out samples where at least one of the meteorological features is NaN. We shuffle Precipitation measurements in each month, and randomly select 10% of the measurements in each month as test-ID and allocate the remaining 90% for training. For OOD testing, all samples in each month are used.

Evaluation Metrics. We evaluate models by their average and worst-time OOD accuracies. The former measures the model’s ability to generalize across time, while the latter additionally measures model robustness to trends in seasonal Precipitation patterns.

Eval-Stream evaluates performance across the next 4 months, which represents 33.3% of all timestamps in the entire dataset and tests a model’s robustness to shifting meteorological measurements from seasonal Precipitation changes.

F.3 Results

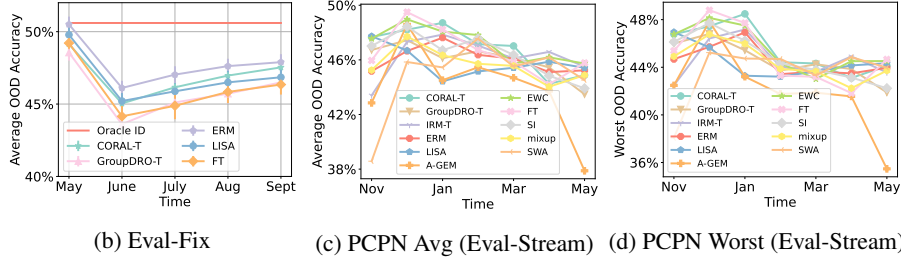
Experimental Setup. We follow [72] and use a FTTransformer [49], which is well-suited for deep learning with tabular data. We use all default architecture settings for the FTTransformer, except that the deep MLP in our FTTransformer has 2 layers, each of size 32 units, and uses LeakyReLU activation.

We use the Adam optimizer with a fixed learning rate of 10^{-3} and train with a batch size of 128. Baselines were trained for 5000 iterations under the Eval-Fix setting and for 500 iterations under the Eval-Stream setting. In terms of hyperparameters for CORAL, GroupDRO and IRM, the CORAL penalty, IRM penalty, learning rate, the number of substreams and the size of substreams are set as 0.9, 1.0, 10^{-3} , 3, 4, respectively.

Results. Similar to Table 12, we reported the results of standard splits and mixed splits and the results of Eval-Stream and Eval-Fix in Figure 10. According to the performance between different splits, we can not observe clear performance gaps between standard split and mixed split. Thus, precipitation

Dataset	Standard Split		Mixed Split	
	OOD Avg.	OOD Worst	OOD Avg.	OOD Worst
Precipitation	46.08%	44.15%	47.56%	45.51%

(a) Performance drops of ERM with different splits on Precipitation dataset.



(b) Eval-Fix

(c) PCPN Avg (Eval-Stream)

(d) PCPN Worst (Eval-Stream)

Figure 10: Results on Precipitation. (b) out-of-distribution performance per test timestamp under Eval-Fix setting; (b) (c): results under Eval-Stream setting.

dataset violates our first dataset selection criterion, and we decide not to include this dataset in the Wild-Time benchmark.

F.3.1 Broader Context

Precipitation forecasting enhances public health, safety, and economic prosperity. Extreme Precipitation warnings can save lives and reduce property damage. Forecasts on temperature and precipitation are crucial to agriculture, and hence to traders on commodity markets. On a daily basis, many people use Precipitation forecasts on a daily basis. Precipitation forecasting comprises a large part of the economy: the United States alone spent 5.1 billion on Precipitation forecasting in 2009, resulting in benefits estimated to be 6 times as much [83].

The Precipitation dataset, which contains heterogeneous tabular data, exhibits data that changes over time due to seasonal changes in Precipitation patterns. In addition, the distribution of the measurement locations are distributed non-uniformly across the planet. Certain climate regions, such as the polar caps, are under-represented, presenting further challenges [72].

G User Guide and Maintenance Plan

G.1 User Guide of Wild-Time

Licenses. The Wild-Time datasets and baselines are freely available for research purposes. Though Drug-BA and Precipitation are not included in the formal Wild-Time benchmark, we still include these datasets in the Wild-Time package. All code for Wild-Time is available under the MIT license. We list the licenses for each Wild-Time dataset below:

- Yearbook: MIT License
- FMoW-Time: The Functional Map of the World Challenge Public License
- MIMIC-IV (Readmission and Mortality): PhysioNet Credentialed Health Data License 1.5.0
- Drug-BA: MIT License
- Precipitation: CC BY-NC 4.0
- Huffpost: CC0: Public Domain
- arXiv: CC0: Public Domain

Hosting Platform. We will use GitHub as the hosting platform of code. We provide (1) detailed data preprocessing scripts to help users process the data from scratch, and (2) preprocessed data from each curated dataset except MIMIC-IV.

Dependencies. Wild-Time is built upon Python 3.8+, and depends on PyTorch, PyTorch Tabular, PyTorch Transformers, PyTDC, Huggingface-Hub. Additionally, it uses numpy, scipy, and scikit-learn for data manipulation.

G.2 Using the Wild-Time Package

In this section, we discuss our open-sourced Python package that provides a simple interface to use the Wild-Time benchmark. Our Python package allows the users to use our datasets with a few lines of code. In addition, users can easily construct their own datasets or baselines on top of our package. Specifically, Figure 11 shows how to use APIs to load the Wild-Time datasets and train a baseline. Beyond the current APIs, we plan to provide standardized evaluation of methods using our dataset in the future.

```
>>> import argparse
>>> from WildTime import dataloader, baseline_trainer
# Load the corresponding config for a specific baseline and dataset
>>> from WildTime.configs.eval_fix.configs_fmow import configs_fmow_ewc
>>> configs = argparse.Namespace(**configs_fmow_ewc)

# If you only need data, you only need the get_data method
>>> fmow_data = dataloader.getdata("fmow", configs)

# If you need to run a baseline, use the following method
>>> baseline_trainer.train(configs)
```

Figure 11: Dataset initialization and baseline training.

G.3 Maintenance Plan

Wild-Time will be maintained by the authors of this paper. The group can be contacted by raising an issue on the GitHub or by writing to the first authors. The dataset is currently hosted on Google Drive storage. The Wild-Time benchmark may be updated at the discretion of the authors. Updates may include adding more diverse baseline methods, datasets, and tasks, or updating infrastructure to improve efficiency. Updates which correct errors will replace previous versions of the datasets.

We welcome contributions to the Wild-Time benchmark. Other parties may update the Wild-Time benchmark by submitting a pull request on GitHub. We are releasing the Wild-Time benchmark under the open-source MIT License. We permit other parties to create new datasets from the Wild-Time benchmark, given that the changes are documented and the Wild-Time benchmark is referenced.

G.4 Author Statement

To the best of our knowledge, the released dataset and benchmark does not violate any existing licenses. However, if such a violation were to exist, the authors claim responsibility for resolving these issues.

H Discussion

H.1 Limitations

One limitation of this paper is that we do not categorize covariant shift and concept drift over time. Though, we've seen some sudden distribution shifts occur in our benchmark, we currently do not find a good way to precisely identify the reasons of sudden distribution shifts and further categorize them. We will focus on this in the next version.

H.2 Ethics Discussion

The Wild-Time benchmark includes the Yearbook dataset, which is an adaptation of the Portraits dataset [26]. The task is binary gender prediction from yearbook photos of American high schoolers. We recognize the harmful ramifications of binary gender prediction. A binary gender prediction task excludes nonbinary individuals, may misgender transgender individuals, and may reinforce problematic gender norms.

The FMoW-Time dataset, adapted from the WILDS benchmark [55], involves geographic region prediction from satellite imagery and has applications to remote sensing. We recognize the privacy and surveillance issues surrounding remote sensing. We remark that FMoW-Time uses a lower image resolution than other publicly available satellite data, such as Google Maps. We also recognize that the FMoW-Time dataset raises issues of systematic bias and fairness. Specifically, the WILDS benchmark [55] found that models performed poorly on satellite images from Africa. As remote sensing is used for development and humanitarian purposes, poor model performance in certain geographic regions can harm certain populations. These issues are discussed in more detail in the UNICEF discussion paper by Berman et al. [6].

The MIMIC dataset, adapted from the MIMIC-IV database [47], involves predicting patient mortality and readmission to the ICU. Ethical challenges associated with using artificial intelligence (AI) in healthcare include (1) informed consent to use, (2) safety and transparency, (3) fairness and algorithmic biases, and (4) data privacy [25]. The MIMIC-IV database adopted a permissive access scheme, allowing for broad reuse of data. With regards to patient privacy, we note that the MIMIC-IV database includes de-identified patient data [47]. We also note that the authors of Wild-Time followed proper credentialing protocol to access the MIMIC-IV dataset. To protect patient confidentiality, we do not release the MIMIC dataset. Instead, we provide instructions for how users can get credentialed on PhysioNet to download the MIMIC-IV dataset and provide a script to generate the MIMIC dataset. We recognize considerations of fairness and algorithmic bias for the MIMIC task. Several studies have found that AI algorithms exhibit biases with respect to ethnicity and gender [74, 79]. Phenotype-related data in healthcare can similarly lead to biased models. This can result in incorrect diagnoses for certain subpopulations, endangering their safety. Finally, we emphasize the importance of robust and interpretable AI, especially in healthcare, where human safety is at stake. We hope that the MIMIC task can help lay the groundwork for further research in this direction. We refer readers to [46] for an in-depth discussion of the ethical issues surrounding AI in healthcare.

H.3 Comments on Designing Temporally Robust Models

In our experiments, we found that most existing approaches can not effectively mitigate natural temporal distribution shifts. We believe that there are two important aspects to consider in resolving natural distribution shift:

- **Learning changeable temporal invariance.** To build a robust model, it would be useful to learn invariance, which captures features in the data that remain invariant across different distributions. However, this is difficult to do when temporal distribution shift happens, as such invariance can also change over time, where one kind of invariance is only suitable for a specific time window. Capturing the correlations between different time windows and determining when and how to update the invariant model are crucial.
- **Leveraging supervised and unsupervised adaptation.** In addition to maintaining a temporally invariant model, adapting to new timestamps is also necessary in tackling temporal distribution shifts. Here, we can leverage labeled data from timestamps in the near past and unlabeled observations from the current timestamp to fine-tune the model. How to combine temporal invariance with supervised and unsupervised adaptation to achieve effective adaptation remains an open problem.

Table 20: The in-distribution versus out-of-distribution test performance of each method evaluated on Wild-Time under the Eval-Fix setting. The average and standard deviation (value in parentheses) are computed over three random seeds. We bold the best OOD performance for each dataset.

	Yearbook (Accuracy (%) \uparrow)			FMoW-Time (Accuracy (%) \uparrow)		
	ID Avg.	OOD Avg.	OOD Worst	ID Avg.	OOD Avg.	OOD Worst
Fine-tuning	95.43 (1.65)	81.98 (1.52)	69.62 (3.38)	47.67 (0.81)	44.22 (0.56)	36.59 (0.98)
EWC	96.36 (0.47)	80.07 (0.22)	66.61 (1.95)	47.42 (0.64)	44.02 (0.65)	36.42 (1.56)
SI	96.40 (0.83)	78.70 (3.78)	65.18 (2.44)	47.41 (0.36)	44.25 (0.97)	37.14 (1.34)
A-GEM	97.18 (0.43)	81.04 (1.40)	67.07 (2.23)	47.09 (0.36)	44.10 (0.65)	36.02 (0.61)
ERM	97.99 (1.40)	79.50 (6.23)	63.09 (5.15)	58.07 (0.15)	54.07 (0.25)	46.00 (0.79)
GroupDRO-T	96.04 (0.45)	77.06 (1.67)	60.96 (1.83)	46.57 (0.57)	43.87 (0.55)	36.60 (1.25)
mixup	96.42 (0.26)	76.72 (1.35)	58.70 (1.36)	56.93 (0.50)	53.67 (0.49)	44.57 (1.02)
LISA	96.56 (0.97)	83.65 (4.61)	68.53 (5.79)	55.10 (0.26)	52.33 (0.42)	43.30 (0.75)
CORAL-T	98.19 (0.58)	77.53 (2.15)	59.34 (1.46)	52.60 (0.10)	49.43 (0.38)	41.23 (0.78)
IRM-T	97.02 (1.52)	80.46 (3.53)	64.42 (4.38)	46.60 (1.40)	45.00 (1.18)	37.67 (1.17)
SimCLR	96.11 (0.92)	78.59 (2.72)	60.15 (3.48)	46.91 (0.65)	44.76 (0.17)	37.00 (0.44)
SwaV	96.24 (0.58)	78.38 (1.86)	60.73 (1.08)	47.31 (0.46)	44.92 (0.81)	37.17 (0.52)
SWA	98.46 (0.15)	84.25 (3.06)	67.90 (4.34)	58.05 (0.14)	54.06 (0.23)	46.01 (0.78)
	MIMIC-Readmission (Accuracy (%) \uparrow)			MIMIC-Mortality (AUC (%) \uparrow)		
	ID Avg.	OOD Avg.	OOD Worst	ID Avg.	OOD Avg.	OOD Worst
Fine-tuning	69.71 (10.8)	62.19 (3.71)	59.57 (4.43)	89.99 (0.98)	63.37 (1.91)	52.45 (2.64)
EWC	77.78 (0.38)	66.40 (0.09)	64.69 (0.01)	89.53 (0.65)	62.07 (1.52)	50.41 (2.03)
SI	71.28 (6.22)	62.60 (3.27)	61.13 (3.39)	89.25 (0.84)	61.76 (0.58)	50.19 (1.25)
A-GEM	73.56 (3.25)	63.95 (0.14)	62.66 (1.23)	88.74 (0.17)	61.78 (0.27)	50.40 (0.51)
ERM	73.00 (2.94)	61.33 (3.45)	59.46 (3.66)	90.89 (0.59)	72.89 (8.96)	65.80 (12.3)
GroupDRO-T	69.70 (4.71)	56.12 (4.35)	54.69 (4.36)	89.22 (0.46)	76.88 (4.74)	71.40 (6.84)
mixup	70.08 (2.14)	58.82 (4.03)	57.30 (4.77)	89.75 (1.04)	73.69 (7.83)	66.83 (11.1)
LISA	70.52 (1.10)	56.90 (0.95)	54.01 (0.92)	89.29 (0.47)	76.34 (8.94)	71.14 (12.4)
CORAL-T	70.18 (4.72)	57.31 (4.45)	54.69 (4.36)	88.77 (0.97)	77.98 (2.57)	64.81 (10.8)
IRM-T	72.33 (1.50)	56.53 (3.36)	52.67 (5.17)	89.49 (0.17)	76.17 (6.32)	70.64 (8.99)
SWA	72.62 (3.60)	59.88 (5.48)	57.68 (6.36)	89.53 (1.96)	69.53 (1.60)	60.83 (2.73)
	HuffPost (Accuracy (%) \uparrow)			arXiv (Accuracy (%) \uparrow)		
	ID Avg.	OOD Avg.	OOD Worst	ID Avg.	OOD Avg.	OOD Worst
Fine-tuning	76.79 (0.51)	69.59 (0.10)	68.91 (0.49)	51.42 (0.15)	50.31 (0.39)	48.19 (0.41)
EWC	76.26 (0.32)	69.42 (1.00)	68.61 (0.98)	51.34 (0.13)	50.40 (0.11)	48.18 (0.18)
SI	76.97 (0.30)	70.46 (0.27)	69.05 (0.52)	51.52 (0.19)	50.21 (0.40)	48.07 (0.48)
A-GEM	77.15 (0.07)	70.22 (0.50)	69.15 (0.88)	51.57 (0.18)	50.30 (0.37)	48.14 (0.40)
ERM	79.40 (0.05)	70.42 (1.15)	68.71 (1.36)	53.78 (0.16)	45.94 (0.97)	44.09 (1.05)
GroupDRO-T	78.04 (0.26)	69.53 (0.54)	67.68 (0.78)	49.78 (0.22)	39.06 (0.54)	37.18 (0.52)
mixup	80.15 (0.17)	71.18 (1.17)	68.89 (0.38)	51.40 (0.20)	45.12 (0.71)	43.23 (0.75)
LISA	78.20 (0.53)	69.99 (0.60)	68.04 (0.75)	50.72 (0.31)	47.82 (0.47)	45.91 (0.42)
CORAL-T	78.19 (0.31)	70.05 (0.63)	68.39 (0.88)	53.25 (0.12)	42.32 (0.60)	40.31 (0.61)
IRM-T	78.38 (0.51)	70.21 (1.05)	68.71 (1.13)	46.30 (0.53)	35.75 (0.90)	33.91 (1.09)
SWA	80.40 (0.22)	70.98 (0.05)	69.52 (0.10)	51.42 (0.30)	44.36 (0.77)	42.54 (0.68)